

①

AD-A286 635



PL-TR-94-2139

ION HEATING PERPENDICULAR TO THE MAGNETIC FIELD

Mats André and Tom Chang

Massachusetts Institute of Technology
Center for Space Research
Cambridge, MA 02139

28 March 1994

Scientific Report No.2

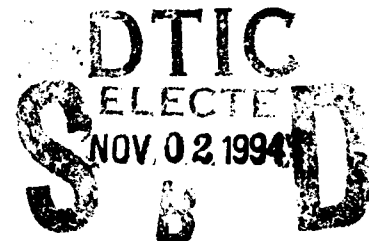
DTIC QUALITY INSPECTED 2

APPROVED FOR PUBLIC RELEASE; DISTRIBUTION UNLIMITED

94-33841



419



PHILLIPS LABORATORY
Directorate of Geophysics
AIR FORCE MATERIAL COMMAND
HANSCOM AIR FORCE BASE, MA 01731-3010

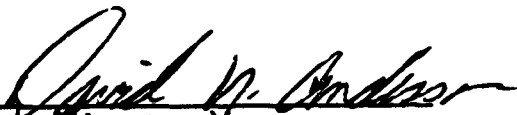
94 11 1 008

"This technical report has been reviewed and is approved for publication"



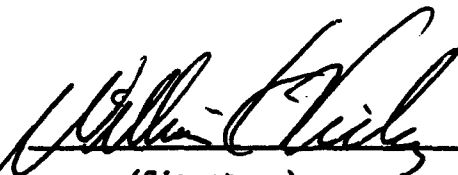
(Signature)

BAMANDAS BASU
Contract Manager



(Signature)

DAVID N. ANDERSON
Branch Chief



(Signature)

WILLIAM K. VICKERY
Division Director

This report has been reviewed by the ESC Public Affairs Office (PA) and is releasable to the National Technical Information Service (NTIS).

Qualified requestors may obtain additional copies from the Defense Technical Information Center (DTIC). All others should apply to the National Technical Information Service (NTIS).

If your address has changed, if you wish to be removed from the mailing list, or if the addressee is no longer employed by your organization, please notify PL/TSI, 29 Randolph Road, Hanscom AFB, MA 01731-3010. This will assist us in maintaining a current mailing list.

Do not return copies of this report unless contractual obligations or notices on a specific document requires that it be returned.

REPORT DOCUMENTATION PAGE

Form Approved
OMB No. 0704-0188

Public reporting burden for this collection of information is estimated to average 1 hour per response, including the time for reviewing instructions, searching existing data sources, gathering and maintaining the data needed, and completing and reviewing the collection of information. Send comments regarding this burden estimate or any other aspect of this collection of information, including suggestions for reducing this burden, to Washington Headquarters Services, Directorate for Information Operations and Reports, 1215 Jefferson Davis Highway, Suite 1204, Arlington, VA 22202-4302, and to the Office of Management and Budget, Paperwork Reduction Project (0704-0188), Washington, DC 20503.

1. AGENCY USE ONLY (Leave blank)	2. REPORT DATE 28 March 1994	3. REPORT TYPE AND DATES COVERED Scientific No. 2	
4. TITLE AND SUBTITLE Ion Heating Perpendicular to the Magnetic Field		5. FUNDING NUMBERS PE 61102F PR 2310 TA G6 WU EA Contract F19628-91-K-0043	
6. AUTHOR(S) Mats André and Tom Chang		7. PERFORMING ORGANIZATION NAME(S) AND ADDRESS(ES) Massachusetts Institute of Technology Center for Space Research Cambridge MA 02139	
8. PERFORMING ORGANIZATION REPORT NUMBER		9. SPONSORING/MONITORING AGENCY NAME(S) AND ADDRESS(ES) Phillips Laboratory 29 Randolph Road Hanscom Air Force Base, MA 01731-3010 Contract Manager: Bamandas Basu/GPIM	
10. SPONSORING/MONITORING AGENCY REPORT NUMBER PL-TR-94-2139		11. SUPPLEMENTARY NOTES	
12a. DISTRIBUTION/AVAILABILITY STATEMENT approved for public release; distribution unlimited		12b. DISTRIBUTION CODE	
13. ABSTRACT (Maximum 200 words) Several theories of ion heating perpendicular to the geomagnetic field are briefly reviewed and assessed. Perpendicular heating of ions leading to the formation of ion conics is common in the ionosphere and magnetosphere. Ion conics at altitudes above a few thousand kilometers are often associated with waves around the ion gyrofrequency. It is concluded that the majority of these ion conics that are locally heated or generated over extended altitude regimes, may be best explained by ion cyclotron resonance heating. At lower altitudes, particularly in the region of discrete auroras, energization by turbulence around the lower hybrid frequency seems to be an important heating mechanism.			
14. SUBJECT TERMS Transverse heating by low frequency waves, Ion heating, Ion conics, Waves around the ion gyrofrequency, Ion cyclotron resonance heating, Energization by turbulence around the lower hybrid frequency.			15. NUMBER OF PAGES 42
16. PRICE CODE			17. SECURITY CLASSIFICATION OF REPORT Unclassified
18. SECURITY CLASSIFICATION OF THIS PAGE Unclassified		19. SECURITY CLASSIFICATION OF ABSTRACT Unclassified	
20. LIMITATION OF ABSTRACT SAR			

CONTENTS

ION HEATING PERPENDICULAR TO THE MAGNETIC FIELD

1.	Introduction	1
2.	Static Electric Field	2
3.	Time-Varying Electric Fields And Cyclotron Resonance	3
	3.1 Resonant Energization	4
	3.2 Cyclotron Resonance Heating	4
	3.3 An Example: Cyclotron Resonance Heating in the cusp	9
	3.4 More About Cyclotron Resonance Heating	14
4.	Heating By Waves Below The Ion Gyrofrequency	15
	4.1 Multiple Cyclotron Resonance Heating	15
	4.2 Subharmonic Heating	17
	4.3 Nonresonant Energization	17
5.	Heating At Higher Harmonics	19
6.	Heating At Low Altitudes By HISS And Lower Hybrid Turbulence	20
7.	Some Additional Examples Of Ion Heating Mechanisms	24
	7.1 Electrostatic Ion Cyclotron Waves	24
	7.2 Trapping by Intense Coherent Waves and Stochastic Acceleration	25
	7.3 Interaction Between Ion Beams	25
	7.4 Heating of Helium in the Equatorial Plane	26
	7.5 Wave Generation and Propagation in the Central Plasma Sheet	26
8.	Parallel Acceleration Associated With Ion Heating	27
9.	Recent Observations By The Freja Satellite	29
10.	Discussion And Conclusions	30

References

Accession For	
NTIS GRA&I	<input checked="" type="checkbox"/>
DTIC TAB	<input type="checkbox"/>
Unannounced	<input type="checkbox"/>
Justification	
By _____	
Distribution/ _____	
Availability Codes	
Dist	Avail and
A-1	Special

ION HEATING PERPENDICULAR TO THE MAGNETIC FIELD

ABSTRACT

Several theories of ion heating perpendicular to the geomagnetic field are briefly reviewed and assessed. Perpendicular heating of ions leading to the formation of ion conics is common in the ionosphere and magnetosphere. Ion conics at altitudes above a few thousand kilometers are often associated with waves around the ion gyrofrequency. It is concluded that the majority of these ion conics that are locally heated or generated over extended altitude regimes, may be best explained by ion cyclotron resonance heating. At lower altitudes, particularly in the region of discrete auroras, energization by turbulence around the lower hybrid frequency seems to be an important heating mechanism.

1. INTRODUCTION

It is well known that ions in the ionosphere and magnetosphere can be heated perpendicularly to the geomagnetic field. These ions may then move adiabatically up the field lines of the inhomogeneous terrestrial magnetic field and form so-called conics in velocity space. These distributions are observed by rockets at altitudes of a few hundred kilometers [1-7] and by satellites up to several Earth radii [8-18]. The observed ion conics have energies from a few eV up to several keV. Much of the heating seems to occur on, or near, auroral field lines. It is now widely believed that heated ions of ionospheric origin can contribute significantly to the magnetospheric plasma [19].

Acceleration parallel to the geomagnetic field can of course contribute to the outflow of ions. The nearly static parallel electric fields that are believed to accelerate auroral electrons downward, can also accelerate ions out into the outer magnetosphere. However, ion distributions with a distinct conical shape in ion velocity space are often observed, indicating that perpendicular or oblique heating is an important phenomenon. Different ion heating mechanisms have been suggested during the past several years [20-24; and references therein]. The purpose of this review is to provide a discussion of some of the mechanisms that have been considered to be important for perpendicular ion heating in the terrestrial ionosphere and magnetosphere.

It is well established that almost all of the energy driving plasma processes in the terrestrial magnetosphere comes from the solar wind. This may be

compared with the magnetosphere of Jupiter where a large fraction of the corresponding energy comes from the rotation of the planet [25; and references therein], or the magnetosphere of a star whose energy comes from fusion processes within itself. Considering the magnetosphere of the Earth, energy originating in the solar wind may eventually cause oscillating electric fields at different frequencies. A large part of the discussions in the literature concerning ion conics is really about what frequency range of electric field oscillations is important for perpendicular ion heating. Possibilities range from nearly static electric fields, to waves with frequencies of the order of the ion gyrofrequency, up to waves above the lower hybrid frequency.

In the following we discuss some possible ion heating mechanisms. These are then compared with observations in an attempt to determine which mechanisms are more relevant. One conclusion is that cyclotron resonance heating is important at high altitudes. Furthermore, energization by turbulence around the lower hybrid frequency seem to be important at low altitudes, particularly in the region of discrete auroras.

2. STATIC ELECTRIC FIELDS

Some electric fields may for all practical purposes be assumed to be constant. This is the case when the ions traverse the region of interest in much less than one field cycle, [26]. An ion in a static homogeneous magnetic field B_0 with an additional perpendicular static electric field E_{\perp} will $E \times B$ drift with an average velocity of $v_d = E_{\perp} \times B_0 / |B_0|^2$ as discussed in many textbooks. Drifts are common in the magnetosphere, e.g., in the cusp/cleft and in the polar cap, [27]. However, such drifting distributions usually can not be confused with the essentially gyrotropic and often more energetic ion conics.

Localized electric fields with strong perpendicular components are common in the auroral zone [26, 28]. Some of these fields might lead to other types of energization processes than $E \times B$ drifts. In an inhomogeneous perpendicular electric field with sharp enough gradient, the ion gyromotion may be disrupted and the ions are then free to be accelerated across the magnetic field [22, 29]. The maximum ion energy achievable by this process corresponds to a velocity with magnitude $|E'/B_0|$, where E' is a characteristic value of the electric field. Note that the ion now keeps this energy if the electric field slowly disappears, in contrast to the $E \times B$ drift in a homogeneous electric field. Another possibility is an oblique electric field that is roughly constant in a limited region in space. The parallel motion of the ions can now transport them into this region of large electric field. In crossing the structure, the ions gain energy equal to the potential drop. However, the increase in perpendicular velocity is again limited by roughly the $E \times B$ velocity obtained from the perpendicular component of the electric field. Ions spending less than one gyroperiod in the electric field may exit with pitch angles near 90° (depending on the angle of the electric field with

respect to the magnetic field), while ions spending longer times in the electric field are likely to end up with more field aligned velocities [22, 30]. Detailed comparisons between data and theory for these types of processes are usually not possible because of the narrowness of the regions of intense electric fields, and the lack of ion data with adequate temporal resolution and sufficient count rates. Note that a static E_{\perp} gives the same v_d to all ions, and thus gives more energy to heavier ions.

3. TIME-VARYING ELECTRIC FIELDS AND CYCLOTRON RESONANCE

The solar wind energy may directly or indirectly generate electric fields over a wide range of frequencies. Frequencies range from below a mHz (micropulsations) up to at least several MHz (the plasma frequency in the lower ionosphere). Many of these fields may be described as linear waves in a homogeneous plasma [31, 32], but nonlinear effects, sharp gradients and transient phenomena are important in numerous situations. Possible generation mechanisms for these electric fields include both microscopic wave-particle interactions (e.g., waves generated by a beam, or by a particle distribution with a loss cone or a temperature anisotropy) and macroscopic phenomena (e.g., Kelvin-Helmholtz instabilities). However, it is not the purpose of this review to provide detailed descriptions of these mechanisms.

If we knew the electric fields for each individual ion along its orbit, we could determine the "exact" ion distribution by integrating the equations of motion for each ion. In practice we know only one or a few field components along the orbit of one, or possibly a few, spacecraft. Above the auroral zone, the velocity of a polar orbiting satellite is often roughly perpendicular to B_0 and thus to the ion orbits. It is often assumed that the fields observed by a spacecraft during a finite time interval is representative for, but not the same as, the fields along the individual ion orbits. Although this is a very common assumption, it is usually not stated explicitly. The time series from a spacecraft is often used to make a power spectrum, using some standard Fast Fourier Transform technique [33, 34]. In the process, details (e.g., phases) of the original observed signal are lost, but this usually is not a problem since we do not want the details of that particular time series anyway. A serious problem, however, is that standard techniques give information about the distribution of wave energy in frequency, but not in wavevector space [34]. Sometimes wavevectors can be estimated [35], e.g., by using a suitable set of measured wave frequency spectra together with dispersion relations derived from the observed particle distributions [36, 37]. Another serious problem is that the obtained frequency spectra may contain significant contributions from essentially static structures that are Doppler shifted to higher frequencies due to the satellite velocity [38, 39]. Keeping these

observational problems in mind, we now proceed to discuss some time varying electric fields that are important for ion energization.

3.1 Resonant Energization

A left circularly polarized wave with frequency equal to the ion gyrofrequency can efficiently accelerate a positive ion perpendicular to a homogeneous magnetic field. Consider an ion in a homogeneous (infinite wavelength) monochromatic left-handed electric field with frequency f equal to the ion gyrofrequency f_c . This electric field rotates in the same direction and with the same angular velocity as the ion. The electric field will apply a constant force on the ion along its orbit, and thus give a velocity increase proportional to the time t , and hence an energy increase proportional to t^2 . This case is similar to the acceleration of ions by a static electric field parallel to B_0 . In this latter case, the resonance frequency can be said to be at zero frequency. Returning to perpendicular energization, we note that a very narrow-banded coherent wave with frequency around f_c is hard to obtain even in a laboratory, and usually do not occur in the magnetosphere. Rather, random phased waves covering a fairly broad frequency band including f_c are often observed. The left-handed component of these waves still interacts efficiently with the ion. However, the ion motion in velocity space can now be regarded as a random walk. The velocity increase is proportional to \sqrt{t} , and the energy increase is thus proportional to t .

Broadband waves at frequencies around and below the ion gyrofrequency are often observed in the magnetosphere [e.g., 13-16, 26, 40-44]. These waves are often associated with transverse ion heating. Thus, both theory and observations seem to indicate that broadband waves around f_c are important for ion heating. Below we discuss some studies showing that such cyclotron resonance heating by waves near f_c is indeed very important for transverse ion energization. This will be followed by discussions involving possible contributions to ion heating from other parts of these broadband spectra.

3.2 Cyclotron Resonance Heating

One simple and efficient ion heating mechanism involves broadband waves around the ion gyrofrequency [41]. Using reasonable assumptions, Retterer et al. [43] applied this cyclotron resonance heating mechanism to observations in the central plasma sheet. In this study, an observed wave spectrum (Figure 1) together with a Monte Carlo simulation were used to produce an ion distribution quantitatively similar to that observed by Winningham and Burch [45] at a geocentric distance of about 2 earth radii (R_E) Figure 2. (The theory predicts that the ions were oxygen ions. This prediction was confirmed by measurements from the mass spectrometer EICS on DE-1 [Peterson, Klumpar and Shelley,

private communications.]) The theory of ion cyclotron resonance heating by broadband waves is based on a diffusion operator. This operator gives the diffusion rate corresponding to the random walk of ions in velocity space. Using the long wavelength approximation, the operator can be written in a very simple form. This approximation should be valid, for example, for broadband Alfvén waves in most regions of the magnetosphere. The appropriate diffusion coefficient is then simply proportional to the electric field spectral density (S) at the local gyrofrequency of the ion species of interest [41, 43]. The resulting average heating rate per ion (Q) can also be shown to be proportional to the spectral density (and thus to the mean square of the electric field fluctuations) at the local ion gyrofrequency [41]:

$$Q = (q^2/2m)S_L \quad (1)$$

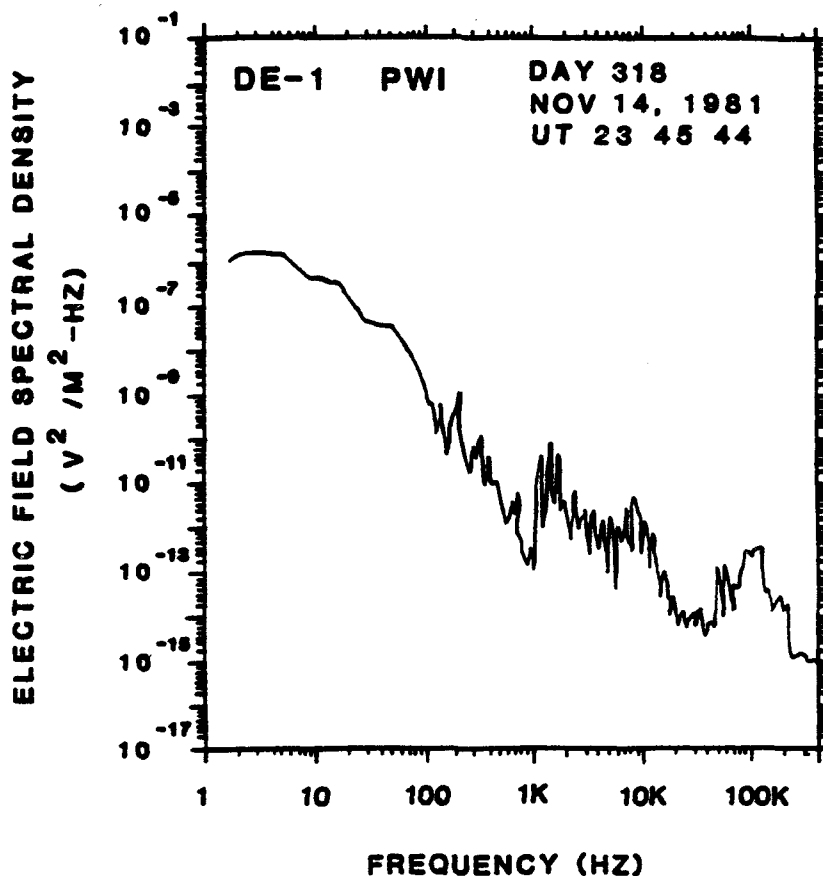


Figure 1. Typical electric field spectral density in the central plasma sheet. Geocentric distance $\approx 2 R_E$, invariant latitude $\approx 60^\circ$. (M. Mellott and D. Gurnett, private communication, 1986)

where q and m are the charge and mass of the ion, respectively. The spectral density, S_L , in equation (1) is the fraction of the spectral density due to left-hand polarized waves. As an example of the relative efficiency of this heating mechanism, we note that a spectral density of $10 \text{ (mV/m)}^2/\text{Hz}$ would yield an average heating rate of 30 eV/s for oxygen ions [13]. This heating rate is high enough to explain ion distributions at essentially 90 degrees pitch angle in the dayside magnetosphere at an altitude of about $13,500 \text{ km}$ (Figures 3 and 4). Figure 5a depicts how an observed wave spectrum may be used to estimate the local ion heating rate.

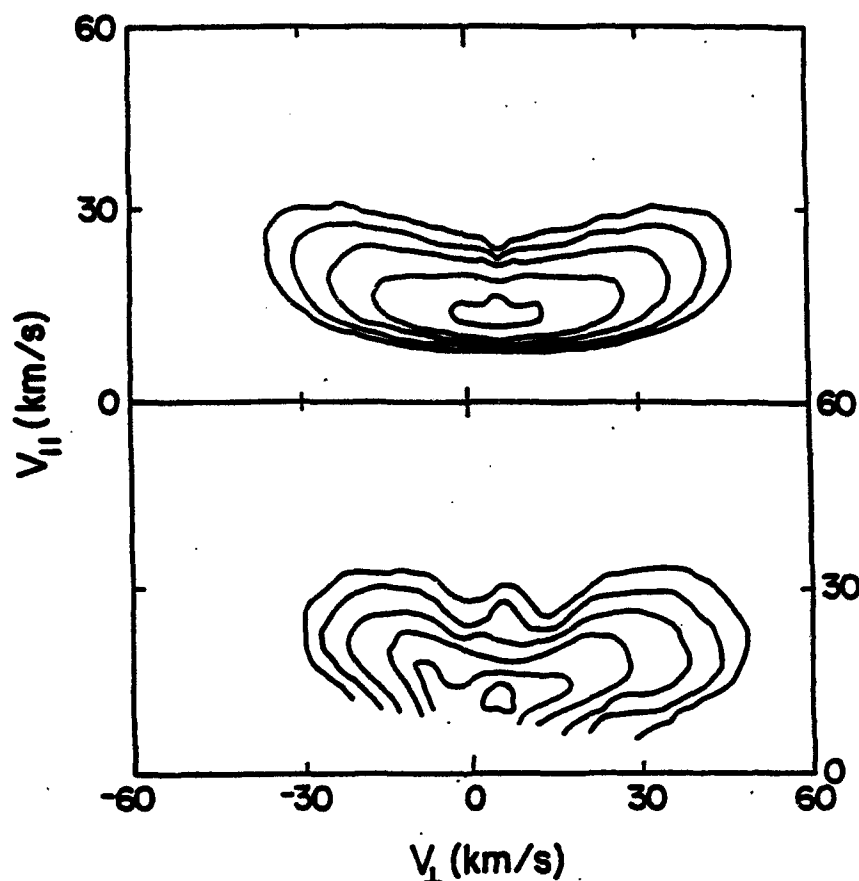


Figure 2. Bottom panel is a contour diagram of the observed ion conic distribution function, measured by the HAPI instrument on the DE-1 satellite (Winningham and Burch, 1984, [45]; the fact that the ions were oxygen ions were confirmed by the EICS instrument on DE-1, Peterson, Klumpar and Shelley, private communications). Top panel is the calculated ion-velocity distribution (Retterer et al., 1987, [43]) using the electromagnetic ion cyclotron resonance theory (Chang et al., 1986, [41]) plotted in the same way as the observed distribution.

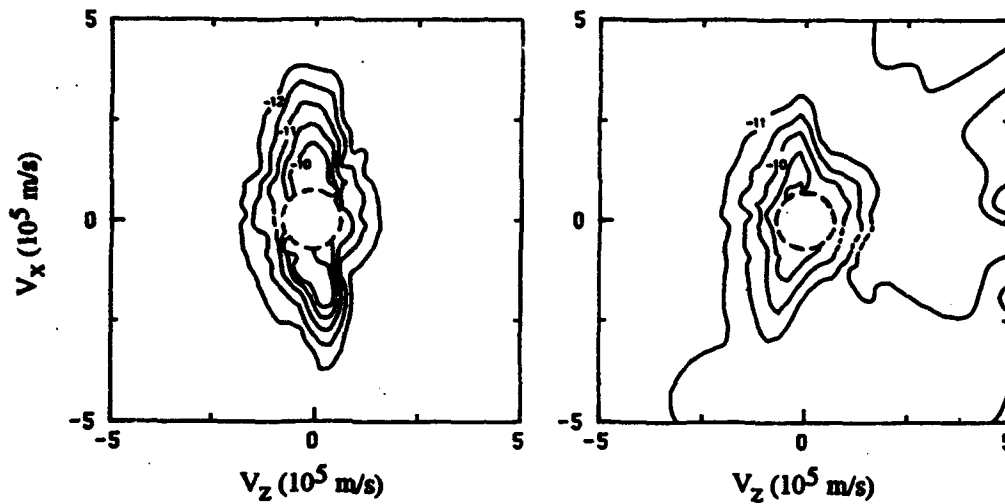


Figure 3. Distribution functions of heated ions observed by the Viking satellite in the cusp/cleft region (André et al., 1988, [13]). The left distribution is obtained near the equatorward edge of the cusp/cleft (2231:14 to 2231:34 UT on July 24, 1986) and is measured simultaneously with the intense broadband waves in Figure 4.

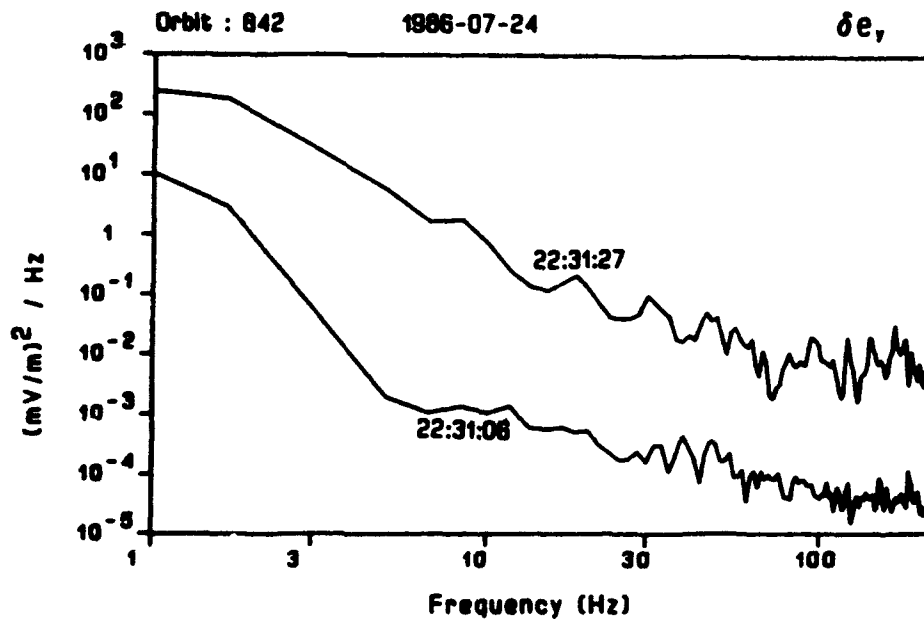


Figure 4. Wave electric field spectra observed by the Viking spacecraft in the cusp/cleft region (André et al., 1988, [13]). The more intense waves (2231:27 UT) are observed simultaneously with the heated ions in Figure 3.

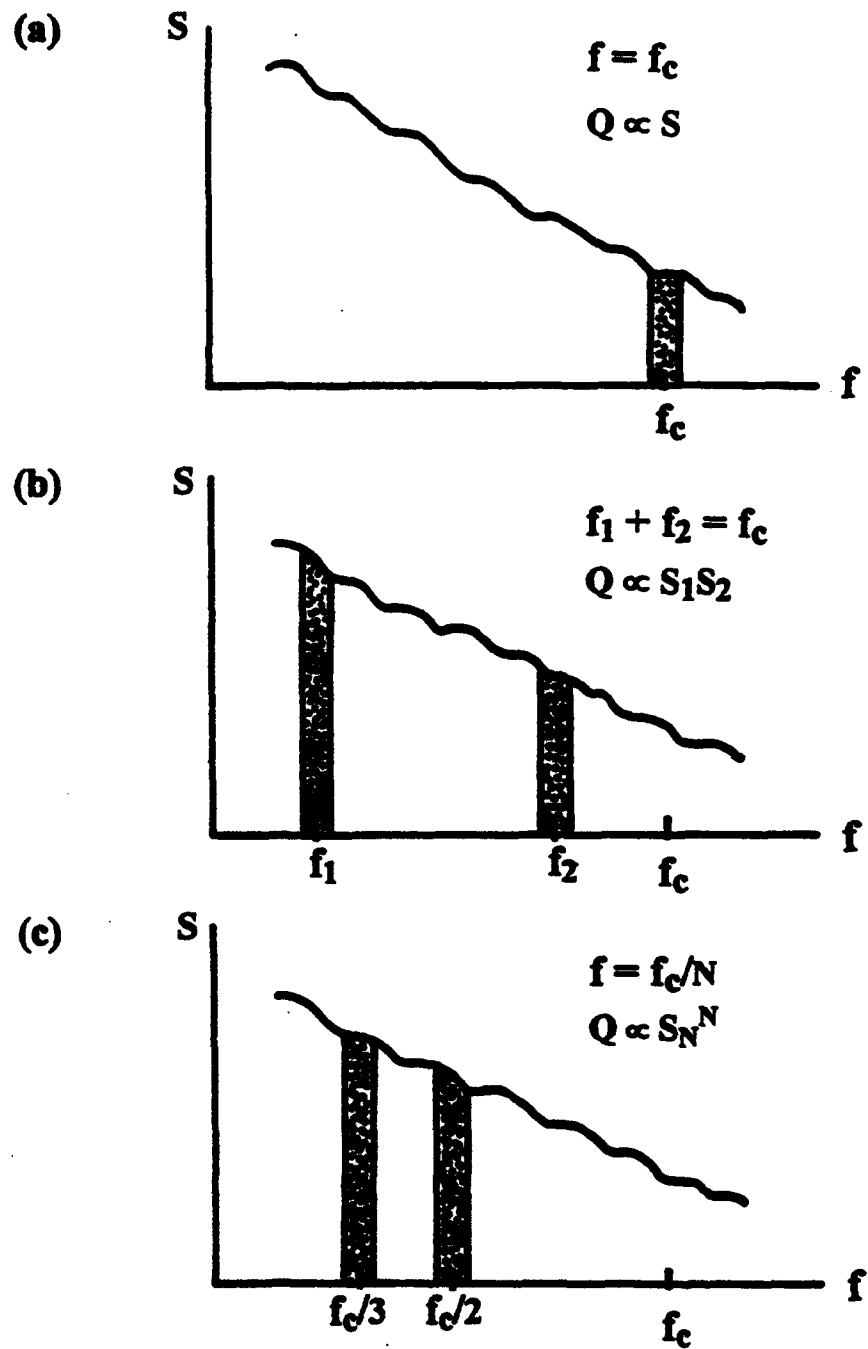


Figure 5. Sketches depicting how an observed wave spectrum can be used to estimate local ion heating by the (a) cyclotron resonance, (b) double cyclotron resonance, and (c) subharmonic resonance mechanisms. Shaded areas depict bandwidths.

Actually the resonance condition $2\pi|f - Nf_c| = k_{\parallel}v_{\parallel}$ should be used to find out at which frequencies (f) ions are in resonance with a wave. Here k_{\parallel} and v_{\parallel} are the parallel wavevector and the parallel component of the particle velocity, while N is an integer. This relation takes into account, e.g., the finite wavelength, and the possibility of interactions at higher harmonics. For emissions with long wavelengths such as most Alfvén waves, the effect of the term $k_{\parallel}v_{\parallel}$ becomes small. Interaction at higher harmonics often require a nonzero perpendicular component of the wavevector.

3.3 An Example: Cyclotron Resonance Heating in the Cusp

As the ions move up the field line, they interact with the spectral densities of different frequency bands as the local ion gyrofrequency changes due to the inhomogeneity of the geomagnetic field. As an example of a test of the cyclotron resonance heating mechanism, we discuss some observations in the cusp/cleft region of the magnetosphere. These studies include mapping of spectral densities down the geomagnetic field, and estimates of the ion heating at various altitudes as these particles move upward [13, 14, 46]. The cusp/cleft is a region of the dayside high-latitude magnetosphere, extending from less than 0900 to more than 1500 magnetic local time and with a latitudinal width of a few degrees [47-49]. In this region, precipitation of shocked solar wind (magnetosheath) plasma usually occurs. Low-frequency broadband waves are also common in this region [50, 51]. A sketch showing a satellite moving poleward into the cusp/cleft region is shown in Figure 6. Here region A is the

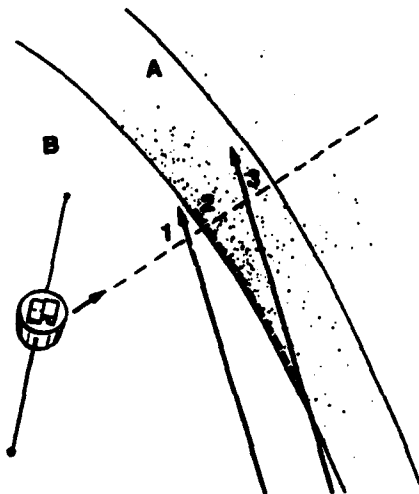


Figure 6. Sketch showing upgoing ions (solid arrows) moving into the cusp/cleft (region A) from the equatorward region (B) due to $E \times B$ convection. Shading in region A indicates low-frequency waves which can heat the ions. From André et al., 1990, [14].

cusp/cleft with rather intense broadband low-frequency waves (shaded), and also with injected magnetosheath particles (not indicated). In the equatorward region B the wave intensity is much lower. Upgoing ions are shown by solid arrows. Since there often is a high-latitude poleward $E \times B$ convection field [52], these ions can drift from region B into region A. A poleward moving satellite may observe upflowing low-energy ions at point 1 in Figure 6. Waves and convection drift can be detected at point 2 and may be mapped down to estimate ion heating and drift at lower altitudes. The heated ions can be observed at point 3.

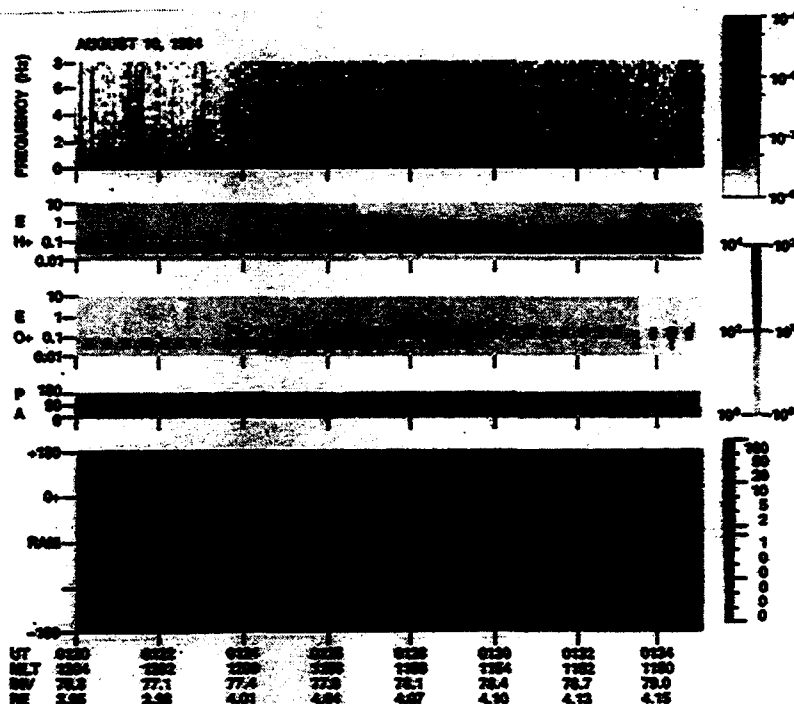


Figure 7. Data from an event where DE 1 moved poleward into the cusp/cleft. The top panel shows electric field spectral density in units of $V^2 m^{-2} Hz^{-1}$ (the O^+ gyrofrequency is 0.85 Hz). The second and third panels show count rates of H^+ and O^+ ions with energies (E) from 10 eV to 17 keV. The left and right scales on the grey bar correspond to the observed H^+ and O^+ count rate, respectively, in counts per sample, which is proportional to number flux. The fourth panel indicates the pitch angle. The bottom panel shows count rate (again in counts per sample) of O^+ ions with energies below 65 eV as a function of spin angle and time, where the solid line indicates the upgoing direction. Note the onset of waves (first panel) and energetic O^+ ions (third panel) at about 0124 UT, and the disappearance of low-energy O^+ ions (lowest panel) at the same time. From André et al., 1990, [14].

Figure 7 shows data from DE-1 obtained when the satellite is moving poleward into the cusp/cleft, i.e., similar to Figure 6. The top panel in Figure 7 shows the low-frequency electric field spectral density. The wave intensity increased after about 0124 UT. In particular, the spectral density at the O^+ gyrofrequency (0.85 Hz) increased, and this is important for the resonant heating we consider. At about 0124 UT the satellite entered the cusp/cleft region, and this corresponds to the edge between region A and region B in Figure 6. The second and third panels of Figure 7 show energy time spectrograms for hydrogen and oxygen. Inside the cusp/cleft, the characteristic hydrogen "butterfly" pattern caused by the poleward $E \times B$ drift of injected ions can be seen [52]. Intense, relatively local heating of upflowing O^+ ions is indicated by the conic-type distributions with a density of roughly 1 cm^{-3} that appear in the third panel at about 0124 UT. It is the heating of these ions we consider in some detail. The bottom panel of Figure 7 shows the counting rate of O^+ ions with energies above the spacecraft potential and below about 65 eV. The data are presented in an angle-time spectrogram format, and indicate that upflowing oxygen ions are present before about 0124 UT. After this time, no low-energy O^+ ions are observed. Comparison with the energetic oxygen spectra in the third panel suggests that the cool O^+ ions are energized out of the low energy region (below 65 eV) after about 0124 UT, i.e., inside the cusp/cleft.

A Monte Carlo simulation has been performed to test the idea of cyclotron resonance heating in detail [14]. The electric fields causing poleward convection and ion heating were observed along the satellite track. Using reasonable assumptions, these electric fields could be mapped down the geomagnetic field. Oxygen ions were then launched at different altitudes along the equatorward edge of the cusp/cleft. Each particle was followed in small time steps up to the satellite altitude. For each time step the poleward drift due to $E \times B$ convection, the upward motion due to the parallel velocity and the adiabatic folding were calculated. In addition, the change in perpendicular velocity due to interaction with waves around the local O^+ gyrofrequency were estimated by using the Monte Carlo technique.

Figure 8 shows the wave input parameters to the simulation together with the energies of the observed and calculated O^+ distributions. The equatorward edge of the cusp/cleft is at about 0124 UT. The middle panel shows the electric field spectral densities at the O^+ gyrofrequency for each satellite spin together with mean values to guide the eye. Points equatorward of the edge are included for comparison. The lower panel shows the spectral indices α (where $S \propto f^{-\alpha}$) used to map the wave intensity to lower altitudes. The upper panel shows the mean energy corresponding to the observed hot O^+ distributions (solid circles) and from the simulation (open). The two curves are in good agreement up to about 0130 UT. After 0130 UT, the east-west drift increases significantly, indicating a turning convection pattern. Thus the problem becomes three-dimensional (particles drifting not only poleward but also eastward), which is

one reason why the agreement between theory and observations is not so good at higher latitudes.

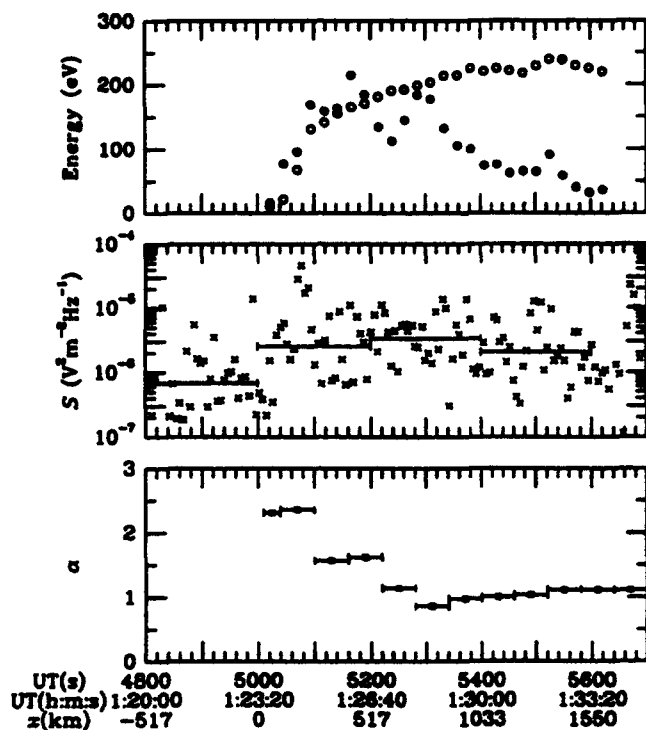


Figure 8. The upper panel shows cusp/cleft O^+ mean energies obtained by DE 1 on August 10, 1984 (solid circles), and from a simulation (open circles) as a function of time (UT given both as seconds after midnight and as hours and minutes). The middle panel shows the electric field spectral density S at the O^+ gyrofrequency. Mean values are also included in this panel. The lowest panel shows the spectral index α . The satellite moves poleward into the cusp/cleft at about 0124 UT where the wave intensity increases and ion heating starts. From André et al., 1990, [14].

Observed O^+ distribution functions are displayed in the upper panel of Figure 9. The left distribution is obtained near the equatorward edge of the cusp/cleft, and seems to be rather locally heated. The right distribution is observed inside the cusp/cleft and indicates more nonlocal heating. Here the ions are more affected by adiabatic folding, and they are more "lifted" in energy toward higher parallel velocities. This is what we expect since these particles have spent more time in the cusp/cleft waves and have traversed a greater altitude range. The lower part of Figure 9 shows the corresponding distribution functions from the simulation. Detailed comparison of these distributions with

the observations is not meaningful since the energy channels of the mass spectrometer are rather wide. However, the simulation distributions show the same tendency as the observations in the sense that the equatorward distribution is more locally heated. Thus there is good agreement between observed O^+ mean energies and distribution functions, and the corresponding O^+ properties obtained from simulations using observed parameters as an input.

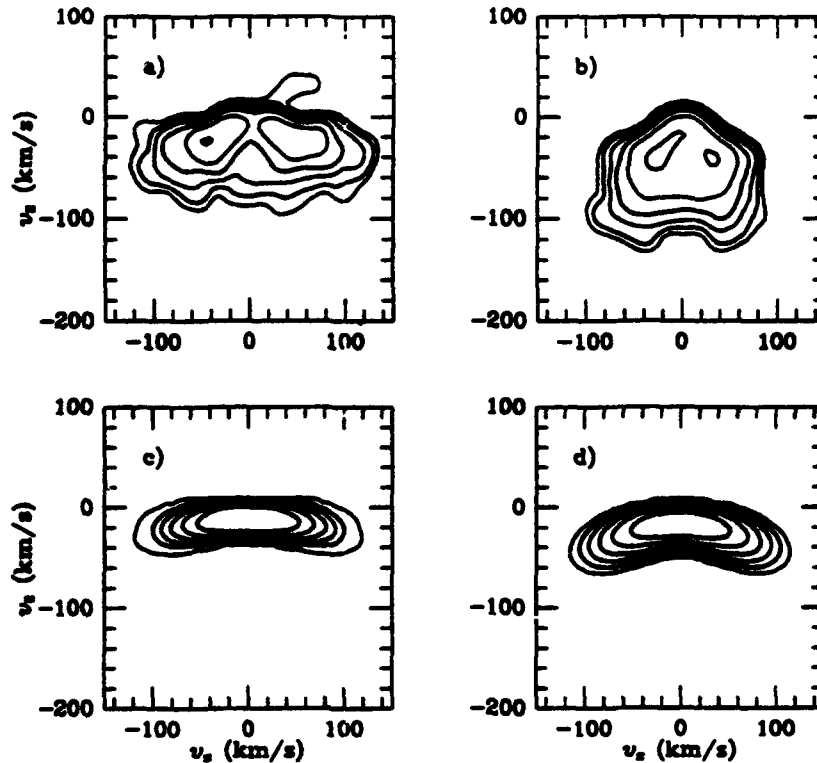


Figure 9. Distribution functions of O^+ ions observed by the EICS mass spectrometer on DE-1 (upper panels) and obtained by a Monte Carlo simulation (lower panels). There are two contours of phase space density per decade, and the innermost (highest) contour corresponds to $2 \times 10^9 \text{ s}^3/\text{km}^6$. The density of the simulation distributions is taken to be 1 cm^{-3} , which is the approximate density of the observed distributions. The left distributions are obtained from 0124:45 to 0126:21 UT, i.e., near the equatorward edge (compare with Figure 8), while the right distributions are from 0128:45 to 0130:21 UT. Note that the equatorward distributions are more locally heated than the distributions from inside the cusp/cleft. From André et al., 1990, [14].

In the above discussion of ion heating in the cusp/cleft we assume that O^+ ions with energies of a few eV exist at altitudes of a few thousand kilometers. These ions are then heated to energies of a few hundred eV on their way up to 10,000 or 20,000 kilometers altitude. This assumption is consistent with conjugate observations of ions by the Akebono satellite ($\approx 5,000$ km) and the DE-1 spacecraft ($\approx 20,000$ km) [53]. Other observations by single satellites confirm the occurrence of ion heating up to a few eV in the low altitude cusp/cleft (see, e.g., ion data below 10 eV from the DE-2 satellite at ≈ 600 km in Plate 2 of Maynard et al. [54]).

3.4 More About Cyclotron Resonance Heating

Careful tests of the cyclotron resonance heating mechanism, involving simultaneously observed wave and ion data, have been performed also in the nightside auroral zone [44]. Here $E \times B$ drifts can often be neglected, and now the heating process may often be characterized by two parameters. These parameters correspond roughly to the velocity and pitch angle of the ion distribution, and may be independently determined from the wave and particle observations of a conic event. The study by Crew et al. [44] again shows good agreement between observations and cyclotron resonance heating theory.

Statistical studies of ion mass spectrometer data from both DE-1 [17] and Akebono [18] indicate that ions are not suddenly heated at one altitude and then adiabatically move upward. Rather, the pitch angles of the ion distributions suggest height-integrated transverse acceleration of ions over a wide altitude range. Again this is consistent with the scenario of cyclotron resonance heating presented above.

We note that no spectral peak around f_c is needed for cyclotron resonance heating to be efficient. Obviously there must be a significant amount of left-handed waves around the gyrofrequency. Often an assumed fraction of about 10% of left-handed waves is sufficient to explain the observed ion heating [14, 41]. The exact wave polarization is hard to determine from electric field observations but the above assumptions seem consistent with magnetometer data [14]. Furthermore, we note that usually no decrease in spectral density around the local f_c is observed. Such a decrease might at first be expected since the waves are transferring energy to the ions. However, it must be realized that only a minor part of the observed wave intensity contributes to ion energization (excluding right-handed waves and electric fields Doppler shifted due to satellite motion). Furthermore, the observed particle energies are often obtained by continuous heating when the ions move thousands of kilometers up the geomagnetic field, corresponding to a wide range of gyrofrequencies. Thus, it is not surprising that observations often show just a broadband wave spectrum associated with ion conics.

Most of the observations discussed above are from altitudes of a few thousand up to about 20,000 km. At first one might expect the O^+ heating rate to simply increase with altitude (decreasing gyrofrequency and thus increasing spectral density in the typical broadband spectrum). At some stage, approximations used in the theory will of course break down. For example, the gyroradius becomes so large that the system can not be assumed to be locally homogeneous. Furthermore, there are indications that the Alfvén wave spectrum has a peak at some small but nonzero frequency. Maximum heating then occurs where this peak matches the local O^+ gyrofrequency. Indeed, observations with good frequency resolution made by the Viking satellite in the cusp/cleft [55] and in the auroral zone [16, 26], and by the Intercosmos-Bulgaria 1300 spacecraft in the auroral zone [56], indicate such a spectral peak between 0.1 and 1 Hz. This corresponds to a maximum heating rate of O^+ ions at an altitude of a few R_E .

At altitudes below a few thousand kilometers, cyclotron resonance heating may be less important simply because the spectral density at the local f_c often is rather low (the gyrofrequency is high). Thus, we conclude that cyclotron resonance heating is important at altitudes from a few thousand kilometers, and at least up to a few R_E . Later we discuss some mechanisms that may be important at low altitudes. First, however, we discuss the possible contribution to ion heating by a broadband spectrum from other frequencies than the gyrofrequency.

4.0 HEATING BY WAVES BELOW THE ION GYROFREQUENCY

4.1 Multiple Cyclotron Resonance Heating

It has been suggested by Temerin and Roth [42] that nonlinear resonance could also produce transverse ion heating. One process involves two waves with finite wavenumbers, where the sum of the frequencies match the gyrofrequency. This mechanism may be called "double cyclotron absorption" (or "double cyclotron resonance"). Assuming low amplitude electric field fluctuations, the average heating rate per ion for this process can be shown to be proportional to the product of the electric field spectral densities at the two frequencies. Although this mechanism is less efficient than ion cyclotron resonance heating (since it is of higher order in spectral densities), it can involve the entire frequency range (below the local gyrofrequency) of the spectrum and can produce a fair amount of transverse ion acceleration, Figure 5b.

Assuming that waves within some bandwidth around half the ion gyrofrequency contribute to double cyclotron absorption, Ball [57, 58] obtained an expression for the average heating rate per ion:

$$Q = (\delta_w/\pi)(5q^2k_{\perp}\eta_{DCA}S_{\Omega/2}/3)^2/(m\Omega)^3 \quad (2)$$

Here $\Omega = 2\pi f_c$, δ_w is the relative bandwidth around half the gyrofrequency over which double-cyclotron absorption is assumed to occur, k_{\perp} is the perpendicular wave number of the waves, $S_{\Omega/2}$ is the electric spectral density around half the gyrofrequency, and η_{DCA} is a dimensionless factor ≤ 1 . The spectral density is assumed to be the same for all frequencies of interest, and thus this spectral density squared occurs in Eq. (2). The derivation of relation (2) requires that k_{\perp} be much less than the inverse of the ion gyroradius and that only waves near $f_c/2$ contribute to the heating. These assumptions seem necessary to obtain a usable expression for the double-cyclotron heating rate, but are not essential features of this heating process. The factor η_{DCA} is included in expression (2) because it is possible that not all the spectral density observed at $f_c/2$ contributes to this heating. As in the case of cyclotron resonance heating, for example, Doppler shift due to the spacecraft motion of spatial electric field structures may occur. We note that double-cyclotron absorption is very inefficient for long wavelengths (small k_{\perp}). The perpendicular wavevector is often very hard to estimate from observations. However, an upper limit of the heating rate given by (2) can be obtained by using a k_{\perp} corresponding to the inverse of the ion gyroradius.

The estimate of the double-cyclotron absorption heating rate in Eq. (2) is a factor of 5 larger than the result given by Temerin and Roth [42]. A possible explanation for this discrepancy is discussed by Ball [57]. However, uncertainties in the estimates obtained from observations of parameters such as k_{\perp} are rather large. Thus the discrepancy between Temerin and Roth [42] and Ball [57, 58] is not sufficiently large to influence an assessment of the possible importance of double-cyclotron absorption as a source of ion conics.

A detailed comparison of double-cyclotron absorption with cyclotron resonance heating in the cusp/cleft region of the magnetosphere was performed by Ball and André [59]. This study included the DE-1 data in Figures 7 and 8, and used the heating rates presented by Ball [57, 58]. It was concluded that double-cyclotron absorption might give an appreciable contribution to O^+ energization, especially when the heating was accomplished locally (in altitude). However, the major conclusion of Ball and André [59] is still that cyclotron resonance heating is the more efficient mechanism for the oxygen conics observed in the cusp/cleft region.

From a theoretical point of view, there exist obviously other higher order resonance processes involving spectral densities at more than two frequencies. However, the heating rates under these circumstances will be of even higher order in wave amplitudes (or spectral densities). For reasonably low wave amplitudes, these higher order effects will be much less efficient and can usually be neglected.

4.2 Subharmonic Heating

From the discussion in the previous section, it follows that waves with frequencies f around the N th order subharmonic ($f = f_c/N$, $N = 2,3,4\dots$) can resonantly heat ions for finite wavelength electric field fluctuations, Figure 5c [42].

The average heating rate is then proportional to the N th power of the electric field spectral density, S_N^N , at the subharmonic. For sufficiently low amplitude fluctuating fields, this indicates the following conclusions: (1) Cyclotron resonance ($N = 1$) is, for typical broadband spectra, often more efficient than subharmonic resonances, (2) 2nd order subharmonic resonance heating (which is equivalent to the special case of double cyclotron resonance for $f_1 = f_2 = f_c/2$) is generally more efficient than those due to other higher order subharmonic resonances, and (3) For broadband electric field spectra, it is more important to include all the double cyclotron resonance effects (in addition to the $N = 2$ subharmonic effect) than to include other higher order ($N > 2$) subharmonic effects.

We end this section by noting that recently Terasawa and Nambu [60] have considered subharmonic ion heating by magnetosonic waves. However, this process requires magnetic fluctuations larger than those usually detected in the auroral and cusp regions.

4.3 Nonresonant Energization

Waves with frequencies much below the ion gyrofrequency may energize ions. Since both the subharmonic heating and multiple cyclotron resonance heating will be of very high order in wave amplitude here, they can generally be neglected. It has been suggested that such waves instead might nonresonantly cause significant ion heating in the magnetosphere [16, 61].

To test this idea of nonresonant energization, Ball and André [59] performed a numerical calculation based on a model of an observed broadband wave spectrum. The upper part of Figure 10 depicts such a model spectrum, constructed by superimposing many sine waves. A spectrum similar to this was observed by the Viking satellite in conjunction with keV protons [15]. The model waves are linearly polarized, and hence include a left-handed component. It was assumed in this calculation that the wavelengths of the fluctuations were very long, $k = 0$, so that multiple cyclotron resonance and subharmonic resonances are not present.

To test the idea of nonresonant heating, the model spectrum was subdivided into three parts: (1) one resonant part (RES) around the proton gyrofrequency at 30.0 Hz, (2) one low frequency (LF) nonresonant part, and (3) one high frequency (HF) nonresonant part. (Thus, the nonresonant part LF contains more than just the very low frequency part.) The effect of the different

parts of the spectrum on ion energization was tested by simply solving the equation of motion for protons subject to the (known) time-varying electric field of the model in the presence of a static uniform magnetic field. The result obtained by averaging over many ions is displayed in the lower panel of Figure 10, showing the mean proton energy versus time. The difference between resonant heating by waves around the proton gyrofrequency and nonresonant energization by other parts of the spectrum is dramatically illustrated. It is seen that the low frequency part of the spectrum causes the perpendicular proton energy to increase rapidly to around 25 eV, after which no further net energy transfer occurs. The energization process due to the high frequency part of the spectrum is similar. The resulting energy is lower, however, since the spectral density is lower there. Estimates show that including wave power at even higher frequencies will not provide much additional ion energization.

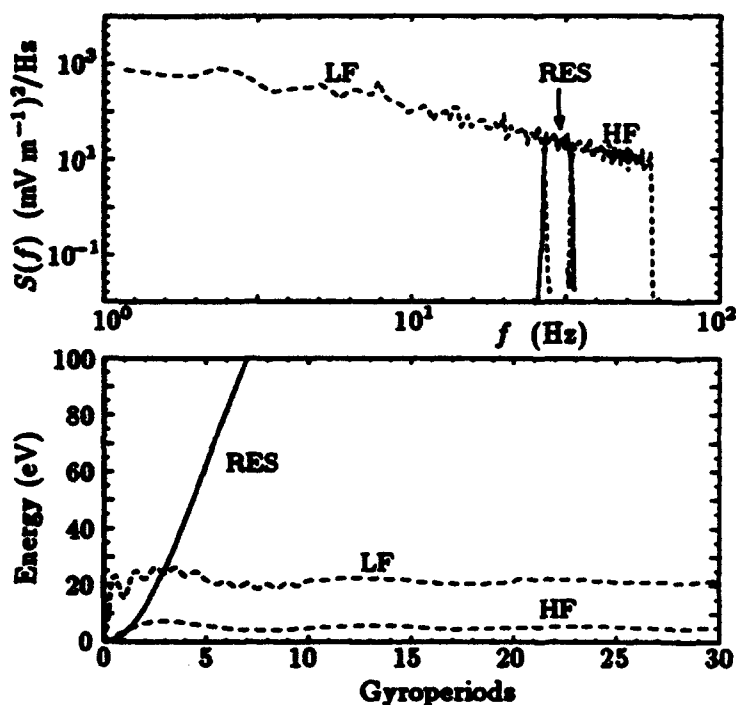


Figure 10. Proton energization due to electric field fluctuations consistent with a spectrum observed together with keV proton conics. The upper panel shows the spectral density calculated from the electric fields used in the numerical calculations. The spectrum has been split into three parts, a resonant part of width $f_c/5$, and nonresonant parts at lower and higher (up to $2f_c$) frequencies. The lower panel shows the average energy of protons subjected to the electric field fluctuations in these frequency regions. From Ball and André, 1991, [24].

The average ion energy Q_δ obtained due to fluctuations in a frequency region δf well removed from f_c , i.e., outside roughly $0.6 f_c < f < 1.4 f_c$, can easily be estimated [59]. A rough calculation includes a static perpendicular electric field of amplitude equal to the intergrated nonresonant spectral density, and thus

$$Q_\delta \approx (2m/B_0^2) \int_{\delta f} S(f) df \quad (3)$$

Here B_0 is the absolute value of the ambient magnetic field. This situation may be compared with a linear oscillator, which is externally driven at a frequency far away from resonance. This oscillator will reach a maximum amplitude, which then does not increase with time.

Returning to Figure 10, we note that after a few gyroperiods the mean proton energy due to resonant heating by waves around f_c is higher than the total energy obtained from nonresonant energization processes. Again we note that no peak in the spectrum around the gyrofrequency is needed for efficient resonant heating, provided sufficient wave power is present near the gyrofrequency.

The numerically obtained heating rate agrees well with the theoretical value from Eq. (1), as discussed by Ball and André [59]. Such resonant heating can readily explain the observed keV protons reported by Hultqvist et al. [15]. On the other hand, nonresonant energization processes can only account for a small fraction of the observed ion energy. We conclude that fundamental ion cyclotron resonance heating can easily explain observed high energy proton conics (above 100 eV) which are hard to explain with any other mechanism.

For events involving heavier ions, the situation is less clear. As discussed above, detailed studies of O^+ heating events show that resonant heating by observed broadband waves can heat the ions to the observed energies. However, since the gyrofrequencies of heavy ions are rather low, it will be more difficult to differentiate the contributions of individual energization mechanisms. At least in some instances, double-cyclotron absorption may significantly contribute to O^+ heating [59]. Similarly, nonresonant interaction with waves below f_c may produce significant O^+ heating [59]. Furthermore, such nonresonant energization may well give high enough energies to explain some ion outflow from the ionosphere [61]. Nevertheless, Ball and André [24, 59] concluded that cyclotron resonance currently provides the best explanation for the majority of observed ion conic events (that are generated either locally or over an extended region in space) at altitudes above a few thousand kilometers in the auroral and cusp/cleft regions.

5. HEATING AT HIGHER HARMONICS

Resonant heating of ions may occur also at higher harmonics of the ion gyrofrequency ($f = N f_c$, $N = 2, 3, 4, \dots$). As in the case of subharmonic heating,

energization at higher harmonics requires finite wavelength electric field fluctuations. Heating at higher harmonics is important, e.g., in energization of Tokamak fusion plasmas with radio frequency waves. Here waves are artificially launched on the magnetosonic branch from the low magnetic field side of the plasma. In the magnetosphere, wave absorption at the second harmonic may be important, e.g., when waves are propagating down a magnetic field line, and thus into a stronger magnetic field [62]. In this situation, the frequency of a downgoing wave will first match the second harmonic before reaching the fundamental gyrofrequency. Indeed, in some cases the downgoing wave may be reflected, e.g., at the ion-ion hybrid frequency, before reaching the gyrofrequency.

Observed structures at higher harmonics of the proton gyrofrequency ($N = 5 - 10$) might be interpreted as evidence of absorption of broadband waves. Ion harmonic structures (lower spectral densities near multiples of f_c) detected by the S3-3 satellite have been suggested as evidence of energy transfer to the simultaneously observed ion conics [63]. However, ion conics may generate emissions between higher harmonics of the ion gyrofrequency, including waves around the lower hybrid frequency [64]. Here the major source of free energy is the positive slope perpendicular to the geomagnetic field in the ion velocity distribution. Thus, harmonic structures may also indicate wave generation rather than wave damping. Structures at upper harmonics of the proton gyrofrequency, above the lower hybrid frequency, have also been observed by the sounding rocket MARIE [86]. Again these structures are not necessarily due to wave damping. The peaks in the spectrum can be H^+ Bernstein modes, generated by, e.g., parametric decay of lower hybrid waves.

For suitable conditions, wave absorption at higher harmonics might be significant. However, for the broadband spectra, which very often are associated with ion conics (see e.g., Figure 1), the wave intensity is much higher at the fundamental ion gyrofrequency than at higher harmonics. Thus, at high altitudes, ion cyclotron resonance heating at the gyrofrequency usually is the more important mechanism.

6. HEATING AT LOW ALTITUDES BY HISS AND LOWER HYBRID TURBULENCE

At altitudes below a few thousand kilometers, cyclotron resonance heating by broadband waves with peaks at very low frequencies may be less important. At these altitudes the spectral density at the local ion gyrofrequency may be rather low. This is simply due to the rapid decrease of spectral density with frequency of the common broadband spectra (see e.g. Figure 1). At low altitudes, there may still be significant ion heating at the fundamental ion gyrofrequency by broadband waves which peak at rather high frequencies. Observations by the AUREOL 3 satellite at altitudes between one and two

thousand kilometers indicate interaction between ions and broadband hiss waves [66]. These waves sometimes show a sharp lower cutoff near the proton gyrofrequency at a few hundred Hz. Details of the emissions near this cutoff has been suggested as evidence of conversion of wave energy from one wave mode to another before ion heating occurs, as discussed in reports by Le Quéau et al. [67] and Le Quéau and Roux [68]. It was noted by Johnson et al. [69-71] that the concentration of the minority ion species must be low (a few percent) for the mechanism discussed in these reports to be significant. Furthermore, at these altitudes the gradient scale lengths may be of the order of the wavelength, and thus, e.g. boundary conditions can become important in estimates of the wave absorption rate.

More narrow-banded waves might, at least in principle, also energize ions. There are some rocket observations of O^+ cyclotron harmonic waves together with perpendicularly heated ions [3]. However, the waves do not seem to be intense enough to explain the observed ion heating.

It seems likely that emissions around and above the lower hybrid frequency are important for ion energization at low altitudes, particularly in the region of discrete auroras. Several years ago, Chang and Coppi [72] suggested that lower hybrid turbulence could be the prime candidate for the transverse acceleration of ions in the high-latitude topside ionosphere, particularly in the region of discrete auroras. Since precipitating energetic electron beams are associated with discrete auroral displays, it was argued that these electron beams could provide the free energy for the production of intense lower hybrid waves that are observed there. The commonly observed geometry of discrete auroras is that the arcs are extended in the longitudinal direction but narrowly confined in the latitudinal direction. This indicates that the region containing the energetic precipitating electrons above a discrete auroral arc (the supraauroral region) must also be similarly confined in the latitudinal direction. The density within the supraauroral region is generally less than that of its immediate neighborhoods with appreciable perpendicular (outward) and parallel (downward) density gradients. The propagation characteristics of the relevant plasma waves that are excited by the energetic electron beam at high altitudes depend crucially on the inhomogeneous density structure of the density depleted supraauroral region. It has been shown by Maggs [73], Maggs and Lotko [74], and Retterer et al. [75], using ray-tracing calculations, that for typical plasma parameters in the supraauroral region, convective modes at frequencies much higher than the lower hybrid frequency will generally propagate out of the region in the latitudinal direction shortly after they are generated. Thus, only those modes close to the lower hybrid frequency, which have group velocities nearly parallel to the magnetic field, can continue to propagate and grow along the field-aligned direction. These lower hybrid modes can stay within the supraauroral region and grow to very large amplitudes leading to the nonlinear coupling and cascading of modes into a broadband spectrum spanning from the original linearly unstable

wavelengths to shorter and shorter wavelengths at lower and lower altitudes [76,77] Figure 11.

It was shown by Retterer, Chang and Jasperse (RCJ) [76] that such type of nonlinear coupling process may be understood in terms of the phenomenon of modulational instability (due to the self-consistently generated low frequency modes) based on the warm fluid approximation for the ions and electrons. In addition to the nonlinear coupling process of wave-wave interactions, concomitant wave-particle interactions control the evolution of the lower hybrid turbulence in the lower altitude magnetosphere and topside ionosphere. RCJ

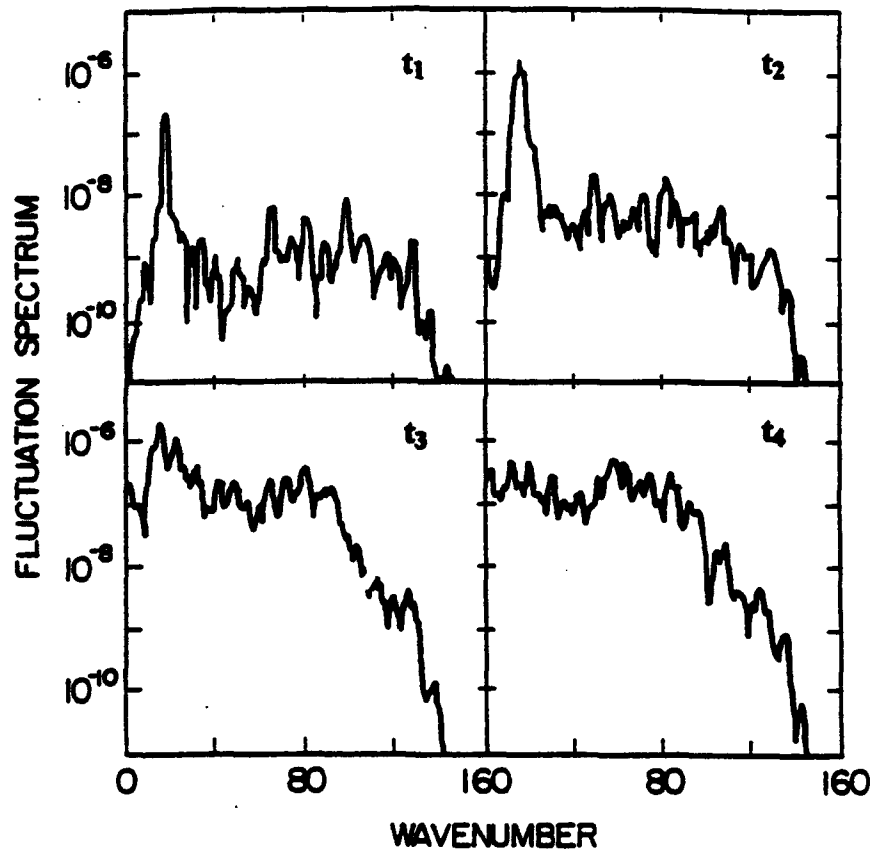


Figure 11. Typical wave spectra from a one-dimensional lower hybrid PIC simulation at four different times with $t_4 > t_3 > t_2 > t_1$. It is seen that the wave energy cascades continually from the k -values of the linearly unstable modes toward larger k -values indicating the cascading process toward shorter wavelength lower hybrid waves. From Retterer et al., 1986, [76].

suggested that the dominant wave-particle interaction process could be modeled by the consideration of instantaneous Landau damping of the waves by the various particle species (i.e., the beam electrons, the background ambient ions and electrons) which at the same time are scattered by the broadband lower hybrid waves through resonant interactions.

Figure 12 depicts the evolution of the amplitude of the electric field in real space and time based on the RCJ model [78, 79]. At the beginning, the

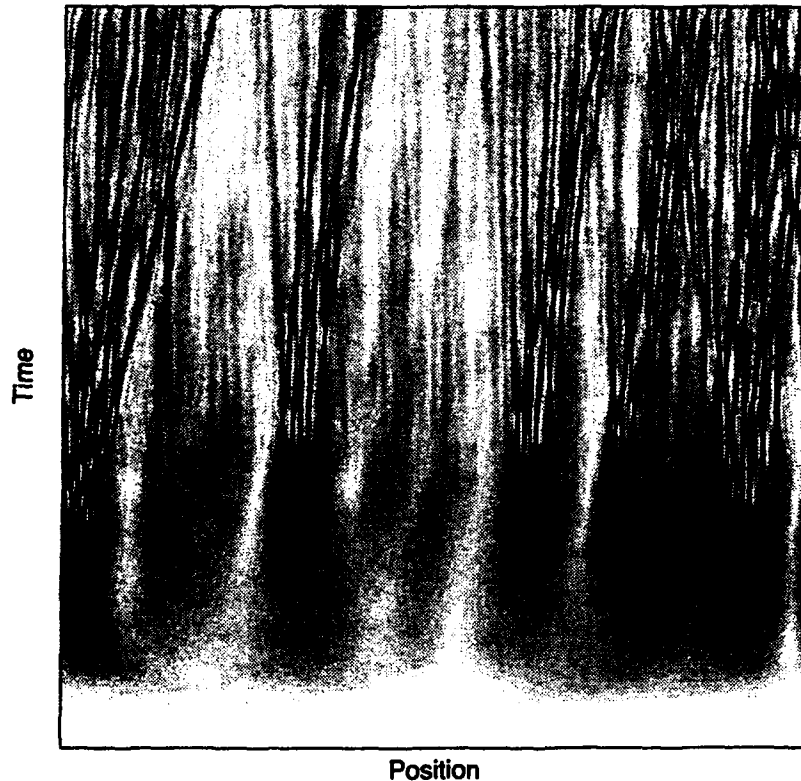


Figure 12. Evolution of lower hybrid caviton turbulence in real space and time based on the RCJ [76] theory. Shading indicates the strength of the electric field amplitude. The horizontal scale is approximately 100 Debye lengths and the vertical scale is approximately 100 ion plasma periods. Notice how the initial nearly uniform wave amplitude intensity evolves into intense individual localized solitary structures or broadband spiky (caviton) turbulence. From Chang, 1993, [79] and Retterer et al., 1993, [78].

amplitude of the electric field grows uniformly. Eventually, when wave cascade sets in, the electric field intensity begins to concentrate aperiodically and in

narrow spatial regions. These localized structures (cavitons, because they correspond to localized density depletions [76, 80]) are seen to propagate at speeds much less than the ambient ion thermal velocity and should appear as stationary structures if detected by in situ electric field measurements. Sometimes these structures are densely mixed forming a spiky turbulence with broadband wavelengths modes. At low altitudes (topside ionosphere; MARIE and TOPAZ altitudes), the individual localized structures that are dominated by short wavelength lower hybrid modes can initiate the transverse energization of ionospheric ions. At mid-altitudes in the supraauroral region (e.g., ISIS-2 or Freja altitudes), the ions energized by the cavitons or other preheating processes can be heated continually by the broadband (spiky) lower hybrid turbulence to higher energies. These broadband lower hybrid waves can also energize the ambient electrons in (both the upward and downward) field aligned directions. The individual localized structures at mid-altitudes, on the other hand, may not find sufficiently cool ions to resonate with. They can, nevertheless, interact with the ambient electrons if the resonant conditions are met, and produce counterstreaming bursts of energized electrons.

Recent rocket experiments [4, 6, 7] have obtained high-time resolution wave-particle data in the topside ionosphere, that are in remarkable agreement with the predictions of the *theories* of Chang and Coppi [1981] and RCJ [1986]. Details of the results of these innovative experiments on the observation of lower hybrid cavitons and associated transverse ion acceleration are given in separate reviews [81, 82].

In addition, the diffusion theory of broadband spiky turbulence of an ensemble of cavitons (or, simply, broadband lower hybrid turbulence) was found to be adequate to explain the observed ion conics by the S3-3 satellite and the MARIE rocket [75]. A diffusion theory based on the idea of combined preheating by cyclotron resonance and continued energization by broadband lower hybrid turbulence has also given a plausible explanation of the recently observed transversely energized ionospheric ion (O⁺) events by the Freja satellite. [See discussions given in Section 10.]

Finally, it is to be noted that lower hybrid waves can be generated by other mechanisms such as ion ring distributions [127], ion drifts [128], and velocity shear [129]. In fact, certain events of transverse ion acceleration observed by S3-3, DE and Freja satellites have been identified with the simultaneous occurrence of precipitating proton and helium rings [127, 130].

7. SOME ADDITIONAL EXAMPLES OF ION HEATING MECHANISMS

7.1 Electrostatic Ion Cyclotron Waves

Several possible ion heating mechanisms in addition to those discussed above have been considered by various authors. One mechanism that has

received considerable attention is heating by electrostatic ion waves above multiples of the ion gyrofrequency. These waves may be generated by simultaneously observed upgoing ion beams, or possibly by drifting electrons [83-87]. Both analytical calculations [e.g., 88] and simulations [89; and references therein], show that electrostatic ion cyclotron waves may cause perpendicular ion heating. However, there is little observational evidence that this energization process is of any major importance in the terrestrial magnetosphere. At high altitudes, these waves are usually observed together with ion beams, rather than ion conics.

There are rocket observations of oxygen cyclotron harmonic waves and perpendicularly heated O^+ ions [3], but these waves do not seem to be intense enough to cause the observed ion heating. However, ion beams may have large perpendicular temperatures (as compared with mean energies in the lower ionosphere), larger transverse than parallel temperature [e.g., 90] and also a vague conic shape [e.g., 86]. This may indicate some perpendicular ion heating by broadband low frequency waves. Furthermore, in many situations the most plausible candidates may be the acoustic waves as investigated by Bergmann et al. [91]. This is further discussed below, in connection with interaction between ion beams.

7.2 Trapping by Intense Coherent Waves and Stochastic Acceleration

When one wave mode dominates the wave field, ion trapping in this mode may occur. In general, the ion trapping orbits will limit the energy achievable by the ions. However, as discussed in a review by Lysak [22], the interactions of the ions with higher harmonics or with other wave modes may allow ions to jump from one trapping orbit to another. This can lead to an irreversible increase in the energy of the ions. For this model to be meaningful, the wave field must be coherent and sufficiently strong [92-94]. The observations of strong, narrowbanded electrostatic ion cyclotron waves within the auroral acceleration region by Mozer et al. [95] motivated Lysak et al. [96], Papadopoulos et al., [97], and Singh et al., [98, 99] to consider stochastic ion heating. However, it is not clear that coherent and intense waves are sufficiently common in the terrestrial magnetosphere for this process to be of any major importance.

7.3 Interaction Between Ion Beams

For several of the ion heating mechanisms discussed in this report, we have not considered the wave generation. In the auroral zone, the situation is rather complex, but one possible generation mechanism is interaction between ion beams. A static potential drop accelerating ions upward will give all ions the same energy, and thus the lighter ions will get higher velocities [100; and

references therein]. Ion beams observed at higher altitudes have much larger temperatures than the source ions [e.g., 90]. Thus, these ions are heated as well as accelerated in the potential structure. One possible source of wave generation and subsequent transverse ion energization are instabilities caused by the relative drift between these ion beams [87, 101-104]. Simulations show that the resulting wave emissions can cause some energization both in the parallel and the perpendicular direction [105-108; and references therein]. Some of the perpendicular heating may be relevant for our understanding of the ion distributions usually called conics. Several other wave generation mechanisms are possible on these field lines. The possibilities include interaction between ion beams and a stationary ion background, electron beams, and various gradients. Thus, again, observations are needed to identify the important wave generation mechanism(s).

7.4 Heating of Helium in the Equatorial Plane

In the equatorial plane near geostationary orbit both wave emissions and their energy source, as well as heated ions, might occur in the same region. Anisotropic, hot proton distributions [109, 110] may generate electromagnetic ion cyclotron waves below the proton gyrofrequency [109, 110-115]. As discussed below, such waves may propagate down to the central plasma sheet. However, the waves may also rather locally heat He^+ ions [112]. We do not expect these helium distributions to have a conical shape, but we include them as an example of transverse ion energization.

In the following section we discuss how waves may propagate from the equatorial plane and cause ion heating at lower altitudes.

7.5 Wave Generation and Propagation in the Central Plasma Sheet

Broadband waves and ion conics are often observed in the region of discrete auroras and in the cusp/cleft region. Here several local energy sources such as sharp gradients and drifting particles can possibly generate some of the waves. However, broadband waves associated with ion conics are also common in the central plasma sheet [41]. As an example of wave generation and transport associated with ion conics we discuss some recent investigations of the central plasma sheet. In this region, equatorward of the region of discrete auroras, there are no obvious local energy sources that can power the broadband waves. This led Johnson et al. [69] to suggest that the waves are generated by anisotropic ion distributions in the equatorial plane. It is well known that left-hand-polarized waves below the proton gyrofrequency can be generated in the equatorial plane. Here a mixture of cool and relatively dense plasma with hot and anisotropic plasma is rather common. The hot ion component often has a higher temperature perpendicular than parallel to the ambient magnetic field

[109], or a significant loss cone [110]. Such a mixture of cool ions and a hot, anisotropic ion population is favourable for the amplification of ion cyclotron waves below the proton gyrofrequency, as discussed by, for example, Cornwall [111]. These waves may then propagate down the geomagnetic field lines. As discussed by Johnson et al. [69], conversion of wave energy from one wave mode to another may be important as the waves propagate downward.

Similar ion cyclotron waves in the plasmopause region have been studied by Horne and Thorne [62], who used ray tracing to study the wave propagation. They emphasized ion cyclotron damping at the second harmonic of the O^+ gyrofrequency. The path-integrated absorption they computed was used to estimate the ion heating qualitatively, but their method did not allow quantitative comparisons based on observed spectral densities.

In a recent study, Rönmark and André [116] discussed the convection of ion cyclotron waves from the equatorial plane to lower altitudes where heavy ions are heated. In this investigation, a model of the equatorial plasma is used to estimate linear wave growth and to model the distribution of wave energy in phase space. Phase space methods developed by Rönmark and Larsson [117] are then used to map spectral densities along the magnetic field lines. The ray tracing methods used by Rönmark and André [116] are rather conventional. However, it is emphasized that the rays are curves in phase space. The conservation of the so called wave distribution function along rays is then used to analyze the transport of wave energy. This method makes it possible to relate the spectral density observed in the ion-heating region to measured spectra in the equatorial plane. The conclusion obtained by Rönmark and André [116] is that wave energy convecting down the field lines in the central plasma sheet can significantly contribute to the waves observed in regions of ion energization.

More recently, Johnson et al. [70, 71] demonstrated that magnetosonic waves could also be ducted from the equatorial region to auroral heights by perpendicular density gradients.

We end the discussion of wave generation and propagation here. In the next section we briefly consider parallel ion acceleration that is often related to perpendicular ion energization.

8. PARALLEL ACCELERATION ASSOCIATED WITH ION HEATING

Ions forming so called ion conics often display characteristics of not only perpendicular but also of parallel energization. This signature consists of field alignment of the ions at energies just above a lower energy cutoff below which essentially no ions are observed (e.g., Figure 2). At increasing energy, the field-aligned distribution gradually becomes a conical one whose apex angle widens with increasing energy. These distributions are sometimes called bimodal, or bowl-shaped, or lifted ion conics. The first discussion of these ion distributions suggested a two stage process [118]. Ions may first be transversely energized,

and then accelerated through a parallel potential drop. It has also been suggested that a parallel electric field that may be decomposed into a fluctuating part and a static part may give similar effects [15, 119]. When E_{\parallel} is changing on a suitable timescale, ions may experience essentially an average downward electric field. The electrons, however, have much larger velocities. These particles may stay in the region of interest during less than one wave cycle, and may be accelerated either upward or downward (given a large enough fluctuating part of E_{\parallel}). Such time-varying E_{\parallel} is one possible explanation of observations of ions and electrons moving upward together. However, we note that the ion acceleration by a parallel electric field does not give perpendicular energization. Thus, the conical shape (distorted by parallel acceleration) has to be explained separately.

It is not necessary to assume parallel acceleration of the whole distribution to cause lifted conics. Rather, the low energy part of the conic may be removed on the way to the point of observation. This might occur via velocity filtering [120]. In this scenario, the ion distribution is transversely bulk heated in some finite region. This process is followed by essentially adiabatic convective flow to the observation location. Here, the latter stage may contribute a velocity filtering effect. Again, the perpendicular heating and the lifting of the distribution in parallel velocity are essentially separate processes.

Some ion heating mechanisms may be described as a random walk in perpendicular velocity. Such a process together with upward motion in a magnetic field with decreasing magnitude, can also give ion conics that are lifted in parallel velocity [121]. Note that only perpendicular energization acting on the whole distribution is needed in this case. At first it may seem strange that a process that accelerates ions only perpendicularly to the magnetic field can produce a distinct low velocity cutoff in parallel ion velocity. However, as discussed by Temerin [121], heating is a stochastic process. That is, though the heated ion distribution always gain energy, individual ions may either gain or lose energy at each time step in the random walk. Ions with small perpendicular velocities observed by a satellite may have reached this spacecraft by moving up the field line through a long heating region. During the time the ions were moving up the field line, they may have gained and lost perpendicular energy several times. During the times they had significant perpendicular energy, they gained parallel velocity due to the magnetic mirror force. Thus, it is extremely improbable that an ion should never have gained any significant perpendicular energy if there are a large number of interactions in the random walk. Hence, all ions should have gained some parallel velocity. As point out by Chang et al. [41] and Retterer et al. [43] and discussed earlier, cyclotron resonance heating by broadband waves is one of the processes that may be described as a random walk in perpendicular velocity. Furthermore, heating over an extended altitude range is needed for lifting in parallel velocity to become obvious. Thus, the cyclotron

resonance heating mechanism is consistent with the observations of lifted ion conics at altitudes above a few thousand kilometers (see e.g., Figure 2).

Recently, Li and Temerin [122] suggested that the pondermotive force derived from the very low frequency portion of the electric field wave spectra can provide field-aligned energization of ions. This idea utilizes the gradient of the $E \times B$ drift in the Earth's diverging magnetic field. The mechanism requires rather large low frequency (much below f_c) fluctuating perpendicular electric fields. A similar process for parallel ion energization in the Earth's nonuniform static electric and magnetic fields was described by Cladis [1986]. Here no explicit time dependence of the fields are introduced in the model. Rather, the parallel ion acceleration is proportional to the $E \times B$ drift and to the rate of turning of the magnetic field direction along the guiding center path of the ion.

Another similar process was discussed by Mauk [124]. In this case a sudden displacement of curved field lines resulting from a short-lived application of an intense electric field may violate the second adiabatic invariant of the lower energy ions. Associated with this violation is the condition that the particles that gain the largest multiplication in their energies are those at small pitch angles. Depending on parameters, this might give significant parallel ion energization.

In some situations these parallel heating processes may need to be considered together with perpendicular ion heating mechanisms when describing the formation of ion conics.

Some recent radar observations at altitudes up to 1500 km indicate significant ion outflows, often associated with auroral arcs [125; and references therein]. These ions have temperatures of a few thousand Kelvin, and field-aligned velocities up to about one kilometer per second. The ion distributions have no obvious temperature anisotropy, and thus are not ion conics. However, these ion outflows can supply particles to regions of perpendicular ion heating at higher altitudes.

9. RECENT OBSERVATIONS BY THE FREJA SATELLITE

The Freja satellite was launched in October 1992 and has an apogee of 1760 km in the northern hemisphere [131]. The Freja orbit with an inclination of 63° is often approximately tangential to the auroral oval, making long continuous observations in ion heating regions possible. Intense ion energization to characteristic energies of up to about 50-100 eV (approximately the same for H^+ and O^+) has been observed on several occasions. These ion conics are often associated with intense lower hybrid waves (with amplitudes up to and above 100 mV/m) but the correlation may be far from perfect. Usually, emissions at low frequencies are also associated with the conics. The ion pitch angles show that most of the heating has occurred within a few hundred km in altitude. One Freja heating event in the eveningside auroral zone has been studied in detail by André et al. [132]. During this event, most of the intense ion heating is probably

caused by the observed lower hybrid waves. These waves may be caused by the simultaneously observed downgoing auroral electrons with energies of several keV. However, some additional energization ("preheating") by e.g., cyclotron resonance heating caused by waves observed around the ion gyrofrequencies (such as that suggested by Chang et al. [133]) seems to be needed. It should be noted that, in contrast to recent observations by sounding rockets, many Freja ion heating events are not associated with individual cavitons [134]. This is consistent with the discussions given in Section 4. The process of modulational instability can produce broadband wavelength lower hybrid waves with or without distinct individual localized structures (or cavitons). This is true irrespective of the generation mechanisms. As asserted earlier, broadband lower hybrid waves and transverse ion acceleration has also been observed in conjunction with precipitating ion rings by Freja [130].

10. DISCUSSION AND CONCLUSIONS

Ion conics are often detected, but simultaneous observations of waves and local transverse heating (ion distributions which peak at 90° pitch angle) by satellites at high altitudes are not common [126]. Such distributions are only occasionally observed at altitudes above a few thousand kilometers [13], although several years of satellite data are available. Some examples of essentially 90° conics have been found by rockets at lower altitudes [4, 5, 6, 11, 12; 82]. However, mechanisms such as electromagnetic ion cyclotron resonance operate over thousands of kilometers in altitude, gradually heating the ions. Thus it is not surprising that only a few locally heated ion distributions have been found at high altitudes.

It seems likely that at least a few different ion heating mechanisms (wave modes) are important in the terrestrial magnetosphere. Future tests of these mechanisms should involve events where more than one heated ion species is observed at a specific time. The heating corresponding to a certain mechanism and ion mass can be estimated from an observed wave spectrum. However, the calculation often involves several assumptions (e.g., about wavelength and wave polarization). Events with more than one ion species should provide even better tests of the theories. Statistical studies of ion conic events where both wave and particle data are available would also help to clarify which mechanisms are important in practice. All these observational studies require high resolution data from, e.g., the auroral zone. One source of such data is the Freja satellite, with an apogee of 1760 km. Thus, this spacecraft can provide a large amount of data from a region where H^+ , He^+ , and O^+ ions are common. Other interesting data will be provided by e.g., the FAST satellite, planned to be launched during 1994, and by sounding rockets. All these data should be used not only to investigate details of the ion heating mechanisms, but also to increase our

understanding of large scale phenomena such as ionosphere-magnetosphere coupling and nonthermal escape of planetary atmospheres.

We have discussed a number of ion heating mechanisms applicable in the terrestrial magnetosphere. At low altitudes, energization by turbulence around the lower hybrid frequency seem to be one important heating mechanism. Some ions that have been perpendicularly heated at low altitudes, may be observed at higher altitudes as upflowing "classical conics" with their vertices located at the origin in velocity space. At altitudes above a few thousand kilometers, cyclotron resonance heating by broadband waves around the ion gyrofrequency seem to be the most important process for transverse ion energization. This mechanism provides bulk heating of the ion distributions. Consequently, the conics resulting from heating over an extended altitude region will generally be lifted in parallel velocity. All these ion heating mechanisms contribute to the outflow of ionospheric plasma into the magnetosphere.

ACKNOWLEDGEMENTS

This research is partially supported by the Swedish National Science Research Council, AFOSR, NASA (Grant Nos. NAG5-2255 and NAGW-1532), AFOSR (Grant No. F49620-93-1-0287) and the Geophysics Directorate of the Phillips Laboratory (Contract No. F19628-91-K-0043). The authors are indebted to R. Arnoldy, L. Ball, B. Basu, Su. Basu, T. Bell, R. Böstrom, J. Burch, S. Chesney, J. Cladis, B. Coppi, G. Crew, C. Dum, L. Eliasson, R. Ergun, A. Eriksson, G. Ganguli, D. Gurnett, M. Hudson, B. Hultqvist, J. Jasperse, J. Johnson, P. Kintner, D. Klumpar, H. Koskinen, R. Pottelette, J. LaBelle, X. Li, W. Lotko, K. Lynch, R. Lundin, R. Lysak, M. Mellott, A. Persoon, W. Peterson, J. Retterer, K. Rönmark, I. Roth, V. Shapiro, V. Shevchenko, W. Tam, M. Temerin, J. Vago, J.D. Winningham, and A Yau for useful discussions and interactions.

REFERENCES

- [1] B. A. Whalen, W. Bernstein, and P. W. Daly, *Geophys. Res. Lett.*, **5**, 55 (1978).
- [2] A. Yau, W. A. Whalen, F. Creutzberg, and P. M. Kintner, in *Physics of Space Plasmas (1985-7)*, SPI Conference Proceedings and Reprint Series, Vol. 6, T. Chang et al., eds. (Scientific publishers, Inc., Cambridge, MA 1987), p. 77.
- [3] P. M. Kintner, W. Scales, J. Vago, R. Arnoldy, G. Garbe, and T. Moore, *Geophys. Res. Lett.* **16**, 739 (1989).
- [4] R.L. Arnoldy, K. A. Lynch, P. M. Kintner, J. L. Vago, S. W. Chesney, T. Moore, and C. Pollock, *Geophys. Res. Lett.*, **19**, 413 (1992).
- [5] G. P. Garbe, R. L. Arnoldy, T. E. Moore, P. M. Kintner, and J. L. Vago, *J. Geophys. Res.*, **97**, 1257 (1992).
- [6] P. M. Kintner, J. Vago, S. Chesney, R. L. Arnoldy, K. A. Lynch, C. J. Pollock and T. Moore, *Phys. Rev. Lett.*, **68**, 2448 (1992).
- [7] J. L. Vago, P. M. Kintner, S. W. Chesney, R. L. Arnoldy, K. A. Lynch, T. E. Moore and C. Pollock, *J. Geophys. Res.*, **97**, 16935, (1992).
- [8] R. D. Sharp, R. G. Johnson, and E. G. Shelley, *J. Geophys. Res.*, **82**, 3324 (1977).
- [9] D. M. Klumpar, *J. Geophys. Res.*, **84**, 4229 (1979).
- [10] D. J. Gorney, A. Clarke, D. Croley, J. Fennel, J. Luhmann, and P. Mizera, *J. Geophys. Res.*, **86**, 83 (1981).
- [11] A. W. Yau, B. A. Whalen, W. K. Peterson, and E. G. Shelley, *J. Geophys. Res.*, **89**, 5507 (1984).
- [12] A. W. Yau, P. H. Beckwith, W. K. Peterson, and E. G. Shelley, *J. Geophys. Res.*, **90**, 6395 (1985).
- [13] M. André, H. Koskinen, L. Matson, and R. Erlanson, *Geophys. Res. Lett.*, **15**, 107 (1988).
- [14] M. André, G. B. Crew, W. K. Peterson, A. M. Persoon, C. J. Pollock, and M. J. Engebretson, *J. Geophys. Res.*, **95**, 20809 (1990).
- [15] B. Hultqvist, R. Lundin, K. Stasiewicz, L. Block, P.-A. Lindqvist, G. Gustafsson, H. Koskinen, A. Bahnsen, T. A. Potemra, and L. J. Zanetti, *J. Geophys. Res.*, **93**, 9765 (1988).
- [16] R. Lundin, G. Gustafsson, A. I. Eriksson, and G. Marklund, *J. Geophys. Res.*, **95**, 5905 (1990).
- [17] W. K. Peterson, H. L. Collin, M. F. Doherty and C. M. Bjorklund, *Geophys. Res. Lett.*, **19**, 1439 (1992).
- [18] W. Miyake, T. Mukai and N. Kaya, *J. Geophys. Res.*, **7**, 11127 (1993).
- [19] C. R. Chappell, *Rev. Geophys.*, **26**, 229 (1988).
- [20] L. Lennartsson, in *Energetic Ion Composition in the Earth's Magnetosphere*, R. G. Johnson, ed. (Terra Publishing Company, Tokyo, 1983), p. 23.

- [21] D. M. Klumpar, in *Ion Acceleration in the Magnetosphere and Ionosphere*, AGU monograph no. 38, T. Chang et al., eds., (American Geophysical Union, Washington, D. C., 1986), p. 389.
- [22] R. L. Lysak, in *Ion Acceleration in the Magnetosphere and Ionosphere*, AGU monograph no. 38, T. Chang et al., eds., (American Geophysical Union, Washington, D. C., 1986), p. 261.
- [23] Tom Chang, G. B. Crew, and J. M. Retterer, *Computer Phys. Comm.*, **49**, 61 (1988).
- [24] L. Ball and M. André, *Geophys. Res. Lett.*, **18**, 1683 (1991).
- [25] J. E. P. Connerney, *Rev. of Geophysics*, **25**, 615 (1987).
- [26] L. P. Block and C.-G. Fälthammar, *J. Geophys. Res.*, **95**, 5877 (1990).
- [27] M. Lockwood, M. O. Chandler, J. L. Horwitz, J. H. Waite, Jr., T. E. Moore, and C. R. Chappell, *J. Geophys. Res.*, **90**, 9736 (1985).
- [28] F. S. Mozer, C. W. Carlson, M. K. Hudson, R. B. Torbert, B. Parady, J. Yatteau, and M. C. Kelley, *Phys., Rev., Lett.*, **38**, 292 (1977).
- [29] K. Cole, *Planet. Space Sci.*, **24**, 515 (1976).
- [30] J. E. Borovsky, *J. Geophys. Res.*, **89**, 2251 (1984).
- [31] T. H. Stix, *The Theory of Plasma Waves*, (McGraw-Hill, New York, 1962).
- [32] M. André, *J. Plasma Phys.*, **33**, 1-19 (1985).
- [33] J. S. Bendat and A. G. Piersol, *Random Data: Analysis and Measurement Procedures*, (Wiley and Sons, New York, 1971.)
- [34] K. Rönnmark, *Space Science Reviews*, **54**, 1-73 (1990).
- [35] J. LaBelle and P. M. Kintner, *Rev. Geophys.*, **26**, 495 (1989).
- [36] T. E. Oscarsson and K. G. Rönnmark, *J. Geophys. Res.*, **94**, 2417 (1989).
- [37] T. E. Oscarsson and K. G. Rönnmark, *J. Geophys. Res.*, **95**, 21187 (1990).
- [38] M. J. Temerin, *J. Geophys. Res.*, **83**, 2609 (1978).
- [39] G. Holmgren and P. M. Kintner, *J. Geophys. Res.*, **95**, 6015 (1990).
- [40] D. A. Gurnett, R. L. Huff, J. D. Menietti, J. L. Burch, J. D. Winningham, and S. D. Shawhan, *J. Geophys. Res.*, **89**, 8971 (1984).
- [41] Tom Chang, G. B. Crew, N. Hershkovitz, J. R. Jasperse, J. M. Retterer, and J. D. Winningham, *Geophys. Res. Lett.*, **13**, 636 (1986).
- [42] M. Temerin and I. Roth, *Geophys. Res. Lett.*, **13**, 1109 (1986).
- [43] J. R. Retterer, T. Chang, G. B. Crew, J. R. Jasperse, and J. D. Winningham, *Phys. Rev. Lett.*, **59**, 148 (1987).
- [44] G. B. Crew, T. Chang, J. M. Retterer, W. K. Peterson, D. A. Gurnett, and R. L. Huff, *J. Geophys. Res.*, **95**, 3959 (1990).
- [45] J. D. Winningham and J. Burch, in *Physics of Space Plasmas (1982-4)*, SPI Conference Proceedings and Reprint Series, Vol. 5, J. Belcher, H. Bridge, Tom Chang, B. Coppi and J. R. Jasperse, eds. (Scientific publishers, Inc., Cambridge, MA, 1984), p. 137.
- [46] W. K. Peterson, M. André, G. B. Crew, A. M. Persoon, M. J. Engebretson, C. J. Pollock, and M. Temerin, in *Electromagnetic Coupling*

- in the Polar Clefts and Caps*, A. Egeland and P. E. Sandholt, eds. (Kluwer Academic, Boston, Mass. 1989), p. 103.
- [47] W. J. Heikkila, in *The Polar Cusp*, J. A. Holtet and A. Egeland, eds. (D. Reidel, Norwell, Mass., 1985), p. 387
- [48] R. Lundin, *Space Sci. Rev.*, **48**, 263 (1988).
- [49] P. T. Newell, and C.-I. Meng, *J. Geophys. Res.*, **93**, 14549 (1988).
- [50] D. A. Gurnett and L. A. Frank, *J. Geophys. Res.*, **83**, 1447 (1978).
- [51] R. E. Erlandson, L. J. Zanetti, T. A. Potemra, M. André, and L. Matson, *Geophys. Res. Lett.*, **15**, 421 (1988).
- [52] J. L. Burch, P. H. Reiff, R. A. Heelis, J. D. Winningham, W. B. Hanson, C. Gurgiolo, J. D. Menietti, R. A. Hoffman, and J. N. Barfield, *Geophys. Res. Lett.*, **9**, 921 (1982).
- [53] W. K. Peterson, A. W. Yau, and B. A. Whalen, *J. Geophys. Res.*, **7**, 11177 (1993).
- [54] N. C. Maynard, T. L. Aggson, E. M. Basinska, W. J. Burke, P. Craven, W. K. Peterson, M. Sugiura, and D. R. Weimer, *J. Geophys. Res.*, **96**, 3505-3522 (1991).
- [55] G. T. Marklund, L.G. Blomberg, C.-G. Fälthammar, R. E. Erlandson, and T. A. Potemra, *J. Geophys. Res.*, **95**, 5767 (1990).
- [56] V. M. Chmyrev, S. V. Bilichenko, O. A. Pokhotelov, V. A. Marchenko, V. I. Lazarev, A. V. Streltsov, and L. Stenflo, *Phys. Scr.*, **38**, 841 (1988).
- [57] L. Ball, *J. Geophys. Res.*, **94**, 15257 (1989).
- [58] L. Ball, *Aus. J. Phys.*, **42**, 493 (1989).
- [59] L. Ball and M. André, *J. Geophys. Res.*, **96**, 1429 (1991).
- [60] T. Terasawa and M. Nambu, *Geophys. Res. Lett.*, **16**, 357 (1989).
- [61] R. Lundin and B. Hultqvist, *J. Geophys. Res.*, **94**, 6665 (1989).
- [62] R. B. Horne and R. M. Thorne, *Geophys. Res. Lett.*, **17**, 2225 (1990).
- [63] D. J. Gorney, S. R. Church, and P. F. Mizera, *J. Geophys. Res.*, **87**, 10479 (1982).
- [64] M. André, M. Temerin, and D. Gorney, *J. Geophys. Res.*, **91**, 3145 (1986).
- [65] P. M. Kintner, J. LaBelle, W. Scales, A. W. Yau, and B. A. Whalen, *Geophys. Res. Lett.*, **13**, 1113 (1986).
- [66] J. L. Rauch, F. Lefeuvre, D. Le Quéau, A. Roux, J. M. Bosqued, J. J. Berthelier, *J. Geophys. Res.*, **98**, 13347 (1993).
- [67] D. Le Quéau, A. Roux, J. L. Rauch, F. Lefeuvre and J. M. Bosqued, *J. Geophys. Res.*, **98**, 13363 (1993).
- [68] D. Le Quéau and A. Roux, *J. Geophys. Res.*, **97**, 14929, (1992).
- [69] J. R. Johnson, T. Chang G. B. Crew and M. André, *Geophys. Res. Lett.*, **16**, 1469 (1989).
- [70] J. R. Johnson, T. Chang, and G. B. Crew, Part I, *Physics of Fluids*, submitted (1993).
- [71] J. R. Johnson, T. Chang, and G. B. Crew, Part II, *Physics of Fluids*, submitted (1993).

- [72] T. Chang and B. Coppi, *Geophys. Res. Lett.*, **8**, 1253 (1981).
- [73] J. E. Maggs, *J. Geophys. Res.*, **83**, 3173 (1978).
- [74] J. E. Maggs and W. Lotko, *J. Geophys. Res.*, **86**, 3439 (1981).
- [75] J. M. Retterer, T. Chang, J. R. Jasperse, in *Physics of Space Plasmas (1989)*, SPI Conference Proceedings and Reprint Series, Vol. 9, T. Chang et al., eds. (Scientific Publishers, Inc., Cambridge, MA 1990), p. 119.
- [76] J. M. Retterer, T. Chang, and J. R. Jasperse, *J. Geophys. Res.*, **91**, 1609 (1986).
- [77] H. Koskinen, *J. Geophys. Res.*, **90**, 8361 (1985).
- [78] J. M. Retterer, T. Chang, and J.R. Jasperse, in *Research Trends in Nonlinear Space Plasma Physics*, R. Sagdeev et al., eds. (American Institute of Physics, New York, N. Y., 1993), p. 252.
- [79] T. Chang, *Phys. Fluids*, **5**, 2646 (1993).
- [80] M. Goldman, *Rev. Mod Phys.*, **56**, 709 (1984).
- [81] J. Vago and P. Kintner, in *Physics of Space Plasmas (1992)*, SPI Conference Proceedings and Reprint Series, Vol. 12, T. Chang and J. Jasperse, eds. (Scientific Publishers, Inc., Cambridge, MA 1993), p. 303.
- [82] R. Arnoldy, K. Lynch, P. Kintner, and J. Vago, in *Physics of Space Plasmas (1992)*, SPI Conference Proceedings and Reprint Series, Vol. 12, T. Chang and J. Jasperse, eds. (Scientific Publishers, Inc., Cambridge, MA 1993), p. 73.
- [83] P. M. Kintner, M C. Kelley, and F. S. Mozer, *Geophys. Res. Lett.*, **5**, 139-142 (1978).
- [84] R. L. Kaufmann and P. M. Kintner, *J. Geophys. Res.*, **87**, 10487 (1982).
- [85] M. André, *Ann. Geophysicae*, **3**, 73 (1985).
- [86] M. André, H. Koskinen, G. Gustafsson, and R. Lundin, *Geophys. Res. Lett.*, **14**, 463 (1987).
- [87] R. Bergmann, I. Roth and M. K. Hudson, *J. Geophys. Res.*, **93**, 4005 (1988).
- [88] E. Ungstrup, D. M. Klumpar, and W. J. Heikkila, *J. Geophys. Res.*, **84**, 4289 (1979).
- [89] M. Ashour-Abdalla and H. Okuda, *J. Geophys. Res.*, **89**, 2235 (1984).
- [90] R. Lundin and L. Eliasson, *Ann. Geophysicae*, **9**, 202 (1991).
- [91] R. Bergmann, P. C. Gray, M. K. Hudson, and I. Roth, in *Auroral Plasma Dynamics*, AGU Monograph, R. Lysak, ed. (American Geophysical Union, Washington, D.C., 1993), to be published.
- [92] G. R. Smith and A. N. Kaufmann, *Phys. Rev. Lett.*, **34**, 1613 (1975).
- [93] C. F. F. Karney, *Physics of Fluids*, **21**, 1584 (1978).
- [94] C. F. F. Karney, *Physics of Fluids*, **22**, 2188 (1979).
- [95] F. S. Mozer, C. A. Cattell, M. K. Hudson, R. L. Lysak, M. Temerin, and R. B. Torbert, *Space Sci. Rev.*, **27**, 155 (1980).
- [96] R. L. Lysak, M. K. Hudson and M. Temerin, *J. Geophys. Res.*, **85**, 678 (1980).

- [97] K. Papadopoulos, J. D. Gaffey, and P. J. Palmadesso, *Geophys. Res. Lett.*, **7**, 1014 (1980).
- [98] N. Singh, R. W. Schunk, and J. J. Sojka, *Geophys. Res. Lett.*, **8**, 1249 (1981).
- [99] N. Singh, R. W. Schunk, and J. J. Sojka, *J. Geophys. Res.*, **88**, 4055 (1983).
- [100] P. H. Reiff, H. L. Collin, J. D. Craven, J. L. Burch, J. D. Winningham, E. G. Shelley, L. A. Frank, and M. A. Friedman, *J. Geophys. Res.*, **93**, 7441 (1988).
- [101] R. Bergmann and W. Lotko, *J. Geophys. Res.*, **91**, 7033 (1986).
- [102] R. L. Kaufmann, G. R. Ludlow, H. L. Collin, W. K. Peterson, and J. L. Burch, *J. Geophys. Res.*, **91**, 10080 (1986).
- [103] P. B. Dusenbery and R. F. Martin Jr, *J. Geophys. Res.*, **92**, 3261 (1987).
- [104] P. B. Dusenbery, R. F. Martin Jr., R. M. Winglee, *J. Geophys. Res.*, **93**, 5655 (1989).
- [105] M. Ashour-Abdalla, H. Okuda, and S. Y. Kim, *Geophys. Res. Lett.*, **14**, 375 (1987).
- [106] I. Roth, M. K. Hudson, and R. Bergmann, *J. Geophys. Res.*, **94**, 348 (1989).
- [107] R. Winglee, R. M., P. B. Dusenbery, H. L. Collin, C. S. Lin, and A. M. Persoon, *J. Geophys. Res.*, **94**, 8943 (1989).
- [108] P. C. Gray, M. K. Hudson, R. Bergmann, and I. Roth, *Geophys. Res. Lett.*, **17**, 1609 (1990).
- [109] D. T. Young, S. Perraut, A. Roux, C. de Villedary, R. Gendrin, A. Korth, G. Kremser, and D. Jones, *J. Geophys. Res.*, **86**, 6755 (1981).
- [110] S. Perraut, A. Roux, P. Robert, R. Gendrin, J.-A. Sauvaud, J.-M. Bosqued, G. Kremser, and A. Korth, *J. Geophys. Res.*, **87**, 6219 (1982).
- [111] J. M. Cornwall, *J. Geophys. Res.*, **75**, 4699 (1970).
- [112] A. Roux, S. Perraut, J. L. Rauch, C. DeVilledary, G. Kremser, A. Korth, and D. T. Young, *J. Geophys. Res.*, **87**, 8174 (1982).
- [113] B. J. Fraser, and R. L. McPherron, *J. Geophys. Res.*, **87**, 4560, 1982.
- [114] T. Oscarsson and M. André, *Ann. Geophysicae*, **4**, 319 (1986).
- [115] R. E. Denton, M. K. Hudson, and I. Roth, *J. Geophys. Res.*, **97**, 12093 (1992).
- [116] K. Rönmark and M. André, *J. Geophys. Res.*, **96**, 17573 (1991).
- [117] K. Rönmark and J. Larsson, *J. Geophys. Res.*, **93**, 1809 (1988).
- [118] D. M. Klumpar, W. K. Peterson, and E. G. Shelley, *J. Geophys. Res.*, **95**, 10779 (1984).
- [119] B. Hultqvist, *J. Geophys. Res.*, **93**, 9777 (1988).
- [120] J. L. Horwitz, *J. Geophys. Res.*, **91**, 4513 (1986).
- [121] M. Temerin, *Geophys. Res. Lett.*, **13**, 1059 (1986).
- [122] X. Li and M. Temerin, *Geophys. Res. Lett.*, **20**, 13 (1993)
- [123] J. B. Cladis, *Geophys. Res. Lett.*, **13**, 893 (1986).

- [124] B. Mauk, *J. Geophys. Res.*, **91**, 13423 (1986).
- [125] J. E. Wahlund, H. J. Opgenoorth, I. Häggström, K. J. Winser, and G. O. Jones, *J. Geophys. Res.*, **97**, 3019 (1992).
- [126] P. M. Kintner and D. J. Gorney, *J. Geophys. Res.*, **89**, 937 (1984).
- [127] J. M. Retterer, T. Chang, J. R. Jasperse, in *Physics of Space Plasmas (1988)*, SPI Conference Proceedings and Reprint Series, Vol. 8, T. Chang et al., eds. (Scientific Publishers, Inc., Cambridge, MA 1990), p. 309.
- [128] J. M. Retterer, T. Chang, J. R. Jasperse, *J. Geophys. Res.*, accepted for publication [1994].
- [129] I. Roth and M.K. Hudson, *J. Geophys. Res.*, **90**, 4191 (1985).
- [130] J.B. McBride, E. Ott, J. Boris, and J. Orens, *Phys. Fluids*, **15**, 2367 (1972).
- [131] H. Romero, G. Ganguli, and Y.C. Lee, *Phys. Rev. Lett.*, **69**, 3503 (1992).
- [132] L. Eliasson, M. André, A. Eriksson, P. Norqvist, O. Norberg, R. Lundin, B. Holback, H. Koskinen, H. Borg, and M. Boehm, submitted to *Geophys. Res. Lett.* (1993)
- [133] T. Stix, *Phys. Rev. Lett.*, **15**, 878 (1965).
- [134] T.F. Bell and H.D. Ngo, *J. Geophys. Res.*, **95**, 149 (1990)
- [135] R. Lundin and G. Haerendel, *AGU Trans., EOS*, **74**, 321 (1993).
- [136] M. André, P. Norqvist, A. Vaivads, L. Eliasson, O. Norberg, A. Eriksson, and B. Holback, submitted to *Geophys. Res. Lett.* (1993).
- [137] A. Eriksson, B. Holback, P. Dovner, R. Boström, G. Holmgren, M. André, L. Eliasson, and P.M. Kintner, submitted to *Geophys. Res. Lett.* (1993).